TRIUMF

ANNUAL REPORT
SCIENTIFIC ACTIVITIES
2000

ISSN 1492-417X

CANADA'S NATIONAL LABORATORY
FOR PARTICLE AND NUCLEAR PHYSICS

OPERATED AS A JOINT VENTURE

MEMBERS:

THE UNIVERSITY OF ALBERTA
THE UNIVERSITY OF BRITISH COLUMBIA
CARLETON UNIVERSITY
SIMON FRASER UNIVERSITY
THE UNIVERSITY OF VICTORIA

ASSOCIATE MEMBERS:

THE UNIVERSITY OF MANITOBA
L'UNIVERSITÉ DE MONTRÉAL
QUEEN'S UNIVERSITY
THE UNIVERSITY OF REGINA
THE UNIVERSITY OF TORONTO

UNDER A CONTRIBUTION FROM THE
NATIONAL RESEARCH COUNCIL OF CANADA

OCTOBER 2001

The contributions on individual experiments in this report are outlines intended to demonstrate the extent of scientific activity at TRIUMF during the past year. The outlines are not publications and often contain preliminary results not intended, or not yet ready, for publication. Material from these reports should not be reproduced or quoted without permission from the authors.

ISAC PROJECT

INTRODUCTION

There has been much activity and many accomplishments in ISAC this past year. The results of this effort are particularly evident in the experimental hall where free space is now at a premium. During 2000, ISAC has been gradually evolving from a construction and commissioning phase towards a fully operational facility. This has implied changes to resource allocation as well as the implementation of new procedures. Operators were trained and given the responsibility of providing radioactive beams to a fully scheduled low-energy science program. With up to 20 μA on target, ISAC has been providing record yields of selected short-lived isotopes for experiments. Yield measurements for some short-lived species indicate unanticipated enhancements as the proton current is increased. The chain of rf accelerating devices and the transport beam line required to provide beams to TUDA and DRAGON are nearing completion. The off-line ion source (OLIS) was used to commission the accelerator components as they became available. A major milestone was achieved on December 21 when a helium beam was accelerated from the OLIS up to full energy (1.5 MeV/u). Progress on the remote handling of the pre-separator slits and the storage vault for spent targets has prepared ISAC for licensing and operation with 100 μA of protons on target. A formal request has been made to the British Columbia Knowledge Development Fund for money to construct the ISAC-II buildings, and procedures have been initiated with the University of British Columbia towards obtaining the required development permits. Meanwhile, development of certain key ISAC-II technology has begun. Formal links have been established with INFN-Legnaro on the construction and testing of a medium-beta superconducting rf resonator structure, and also with ISN-Grenoble on measuring the performance of a charge state booster (1+ to n+ CSB) based on an electron-cyclotron-resonance ion source.

ISAC OPERATIONS

This year was one of transition between commissioning and operation of the ISAC-I low energy facility. Four new operators and a target hall coordinator were hired in the first quarter. Intensive training was provided in the last few weeks of April by way of more than 30 hours of formal lectures (a result of approximately 200 hours of preparation time for the lecturers). The lectures were videotaped for future use in the training of new operators. This training was introductory and should be considered as the first iteration of a training program which will be developed as a “systems approach to training” (SAT). In early May, after this initial training, the new operators were assigned to shift work and began coverage of ISAC beam production. Unfortunately, one of the new recruits left in June to accept a position closer to his home in the Okanagan. Two replacement operators were hired in October, and had received their orientation and introductory training by the end of the year. Thus, at year end, the group was composed of ten members: the head of ISAC operations, a training and documentation coordinator, seven operators including new personnel (Chris Payne, Harvey Quan, Saeideh Yeganeh, Rene Tanaja and Travis Cave), and, finally, a target hall coordinator, John McKinnon.

Less reliance was made on beam physicists during routine beam operation, although their assistance is always a welcome benefit. Their efforts have been more devoted to studying the beam reproducibility, and during commissioning of each new target they have been available to optimize the beam through the mass separator (especially the emittance) and to measure target yields.

During periods of extended maintenance, the ISAC operators have been available to assist with maintenance and other ISAC activities such as the installation of new facilities. In the target hall, much progress was made in preparing the facility for regular service. The boot change area was set up with radiation monitoring equipment and stocked with supplies of protective clothing. Special tool cabinets and work areas were set up in the hall, and the procedures for disconnecting the target services and transporting targets between the target station and the hot cell were developed.

This year, for the first time, operational performance statistics are provided for the ISAC beam production. It should be noted that as a single user facility of radioactive ion beams (RIB), there is an incentive to minimize activation when the beam is not required. This is done by stopping the RIB on a Faraday cup in the target station and, for longer periods, turning off the proton beam. For operations purposes, these appear as OFF time for each experiment. Some of this OFF time may be due to a cool down period during an acquisition cycle, or overhead for the experiment such as changing of samples or collection tapes. Therefore some care must be taken in using these statistics for analyzing the scheduled experiment beam time usage.

Table XIX gives the down time for each ISAC system and overhead for operational activities. For most systems, the down time is a sum of many different problems, e.g. for controls, related to the PLC hardware and EPICS program. The magnet power supply time results mostly from a single event in which the mass separator power supply developed a water leak. "Beam line 2A unavailable" indicates times when the proton beam was off for a variety of reasons, including scheduled cyclotron maintenance. "ISAC idle" includes time when the proton beam may have been available but, in the absence of system failures, ISAC RIB was not delivered, e.g. when trained operators were not available or experiments were unable to take beam.

ISAC Beam Statistics for Beam Schedules 97 and 98

Table XIX. ISAC systems downtime and overhead for beam schedules 97 and 98.

ISAC system	Hours
Controls	78.20
Diagnostics	0.50
Magnet power supplies	63.60
OOPS	16.15
Safety	1.20
Services	1.65
Site power	9.40
Vacuum	2.75
OTHER	
Beam line 2A unavailable	964.50
ISAC cooldown	57.05
ISAC idle	188.05
ISAC startup	38.55
ISAC maintenance	1.00
Target/ion source conditioning	145.80
Procedures	40.40
Operator training	9.30
LEBT tuning	352.10
Target changes	92.50
Yield measurements	19.35
TOTAL	2,082.05

The history of operation of ISAC production targets is given in Table XX. Several target changes were done this year. The first ever target change scheduled during beam production, utilizing the target hall remote crane and newly commissioned hot cell facility, occurred in June. A target composed of niobium foils for the production of rubidium beams was replaced with a target of tantalum foils for the production of gallium and lithium beams. Although the planned procedures were followed, some cross contamination of residue in the target module containment box onto the exterior of the target module, most likely via the manipulator grippers, resulted in a minor spread of contamination in the target hall. The predominant species were ^{83}Rb and ^{85}Sr. The hall was cleaned up and several contamination control steps were added to the procedures. As a result, there were no incidents of contamination in the subsequent target changes. In July, the tantalum target was replaced with one of compressed calcium zirconate pellets for potassium and rubidium beams, then in October a target of silicon carbide pellets was installed for production of lithium beams. Until the second target station is commissioned, the turn around for a target change is about ten days which includes a two day cool down period, five days to effect the change and three days for conditioning of the new target.

The members of the ISAC Operations group take great pride in their contributions to the successes of the major ISAC milestones which were achieved this year and have been highlighted elsewhere in this Annual Report. RIB was available for 2,478.95 hours (1,872.85 + 155.55 + 450.55). The combined cyclotron/ISAC performance was 66.2% (2478.95/3745.00). All scheduled experiments received enough beam to satisfy their

Table XX. ISAC target history.

Target ID	In date	Out date	Charge μAh	Thickness g/cm^2	Power μAh $\times$ g/cm^2	Comments
CaO #1	25-Nov-98	15-Dec-98	70	36.00	2,520.0	Failure due to EE short
CaO #2	20-Dec-98	15-May-99	363	31.10	11,289.3	Failure due to EE short
Nb foils #1	14-Jul-99	20-Oct-99	3,242	11.10	35,986.2	Failure due to TBHT-t/c problem
Nb foils #2: R1	01-Nov-99	09-Dec-99	3,149	11.50	36,213.5	Removed for 100 μA tests
Dump only	10-Dec-99	10-Dec-99	43	0.00	0	100 μA test
Talbert	17-Dec-99	12-Jan-00	197	10.00	1,970.0	100 μA test
Nb foils #2: R2	17-Mar-00	04-Jun-00	5,913.8	11.50	68,008.7	Total: Nb foils #2 R1 + R2
Ta foils #1	10-Jun-00	19-Jul-00	3,515.83	21.25	74,711.4	Removed for $CaZrO_3$
$CaZrO_3$ #1 R1	24-Jul-00	21-Aug-00	518.7	42.27	21,925.4	9.45 g Ca/cm^2, 21.51 g Zr/cm^2
$CaZrO_3$ #1 R2	02-Oct-00	18-Nov-00	838.0	42.27	35,422.3	9.45 g Ca/cm^2, 21.51 g Zr/cm^2
SiC #1 R1	18-Nov-00		2,174.0	7.43	16,152.8	7.43 g SiC/cm^2: 5.05 g Si/cm^2, 2.38 g C/cm^2

commissioning milestones and preliminary experiment requirements. The RIB delivered to experiments is shown in Tables XXI and XXII. In the coming year, in addition to providing beam for the scheduled experiments and performing systems maintenance, the major effort will be to establish and complete the SAT training program for ISAC operators, which includes systems operation manuals.

Table XXI. Beam time available to ISAC experiments (hours).

Experiment #	Scheduled	Actual	Tune	Off
E715 (TRINAT)	912.00	606.25	14.10	55.30
β-NMR commissioning	660.00	351.90	41.75	44.80
E815 (β-NMR)	168.00	156.20	11.65	16.85
E801 (GPS1)	204.00	124.70	12.65	16.70
E823 (GPS1)	480.00	317.15	2.45	47.70
E823 (GPS2)	156.00	128.90	7.35	7.05
E826 (LTNO)	72.00	27.50	2.50	24.80
E828 (LTNO)	409.00	19.75	9.45	193.70
E863 (LTNO)	132.00	1.10	8.60	1.00
E841 (YIELD)	516.00	139.40	45.05	42.65
Mass separator development	36.00	0.00	0.00	0.00
TOTAL	3,745.00	1,872.85	155.55	450.55

Table XXII. Radioactive beams delivered to ISAC experiments (hours).

Isotope	E715 TRINAT	β-NMR Comm.	E815 β-NMR	E801 GPS1	E823 GPS1	E823 GPS2	E826 LTNO	E828 LTNO	E863 LTNO	E841 Yield	Total
^{7}Li*		17.55								1.55	19.10
^{8}Li		334.35	156.20							2.55	493.10
^{14}N*									1.10^{+}		1.10
^{26}Na										15.15	15.15
^{36}K										3.15	3.15
^{37}K	60.35				0.50					4.30	65.15
^{38}K	544.00				123.50					3.60	671.10
^{39}K*	1.90				0.85			6.60			9.35
^{64}Ga										0.40	0.40
^{74}Ga					1.15						1.15
^{75}Ga										0.90	0.90
^{76}Ga										0.45	0.45
^{74}Rb					180.65	94.75				18.95	294.35
^{75}Rb					10.50					3.90	14.40
^{79}Rb								13.15			13.15
^{80}Rb						34.15					34.15
^{85}Rb*										7.70	7.70
^{87}Rb*										0.40	0.40
^{91}Rb							27.50				27.50
^{133}Cs										0.50	0.50
^{162}Yb				124.70							124.70
Other										75.90	75.90
Total	606.25	351.90	156.20	124.70	317.15	128.90	27.50	19.75	1.10	139.40	1,872.85

* stable beam $^{+}$ from OLIS

CONVENTIONAL FACILITIES AND INFRASTRUCTURES

The year 2000 was the last of the 4 year construction effort for ISAC! TRIUMF's endeavour to have the new ISAC beam line operational as per schedule demanded continued and focused support from the Infrastructure group. In the next fiscal year, ISAC-I will be a fully operational facility. However, construction activities will continue with the newly approved ISAC-II expansion project. Close coordination work continued with the Accelerator group, the Engineering group and the Science Division. This included attendance at regular and engineering meetings and participation in engineering design reviews and maintaining the as-built arrangement drawings. The Data Network continued to expand to accommodate the new experimental stations.

Once the β-NMR facility was completed, the focus of the installation shifted towards the services for the high-energy beam lines and the remaining infrastructure in support of the experimental program. The gas handling facility and a liquid nitrogen facility were installed late in the year. Maintenance was carried out with the help of the Plant group. A few problems surfaced in the mechanical services but they were promptly corrected. Discussion started on the functional requirements to be incorporated in the ISAC-II project and a preliminary building concept was prepared. Preliminary engineering and cost estimates were provided for ISAC-II. Assistance was provided for the ISAC operators training program.

Building Services

A significant effort was given to support the building services requirement for ISAC. Major projects included:

- A radiation shield at the DTL portion of the high-energy beam consisting of a 24 ft long $\times$ 12 ft wide $\times$ 11 ft high steel beam structure to support 18 removable composite lead on plywood panels.
- A 16 ft long $\times$ 12 ft wide $\times$ 9 ft high data acquisition cabin for the TUDA experimental facility. The cabin was built in conventional wood stud construction with vinyl coated gypsum panels on the outside and plywood on the inside. All internal surfaces were covered with a copper sheet to provide insulation from RFI noise. Dissipative tiles were installed on the floor to prevent excessive static buildup.
- An 18 ft long $\times$ 12 ft wide $\times$ 9 ft high gas storage and handling facility was installed adjacent to the east wall of the experimental hall to provide the experimental program with its gas requirements. This building is also of conventional wood stud construction with pre-finished metal siding panels on the outside and painted drywall inside. The roof deck is made of two-ply torch-on membrane. An explosion proof exhaust fan ensures the evacuation of volatile gases from this room.
- A liquid nitrogen tank was placed next to the gas handling facility.
- The sectional east hatch in the experimental hall was redesigned and replaced with a single 9 ft $\times$ 7 ft $\times$ 12 in. reinforced concrete block for ease of access to the target hall and hot cell areas.
- The access to the target hall was also redesigned to implement a radiation control zone. The new area includes washable walls, vinyl floor, sink, a worker change area and boot boxes.

Electrical Services

The installation of services in the experimental hall continued at a fast pace throughout the year. On the design front, we were very busy with finishing the β-NMR services, and continuing the design for the DTL, HEBT, DRAGON and TUDA services. Design is still in progress for the 8π station. An elaborate, electrically shielded data acquisition cabin and a single-point signal reference scheme were engineered for TUDA along with a high-isolation transformer to minimize electrical interference and disturbances to the very sensitive detector electronics.

Major tasks for the year included the installation of the dc and ac power distribution, racks for beam line power supplies, controls and diagnostics, and cable tray systems and grounding for the following systems/areas:

- β-NMR 60 kV station.
- DTL.
- Safety. Conduit runs installation for the radiation safety monitoring system in the HE experimental area. Support for the sequence and interlocks for exclusion areas and high voltage stations.
- DRAGON experimental station.
- TUDA experimental station.

The services for DRAGON, the second leg of HEBT and the gas handling facility are still in progress and will be commissioned in February, 2001.

Mechanical Services

Most of the site mechanical service engineering effort went into projects in the high-energy area of the experimental hall. Notable jobs included: assembly and services for fume hoods; new compressor for chiller CH-1; new transmitter and remote control for the experimental hall crane; piping of cooling services for MEBT, HEBT, DTL, DRAGON and TUDA; DRAGON hydrogen vent; air conditioning for the TUDA data acquisition cabin; assembly of TRINAT cooling water return system; high level alarms for decontamination sump filling points; charcoal filter for target hall vacuum pump exhaust; breathable air supply in the target hall; perimeter drainage sump pump piping; and laminar flow diffusers for TRINAT. Estimates were given for the superconducting rf cavity assembly and test facility. Calculations for HEBT buncher water flow were provided and consultation provided for DTL cooling problems.

SAFETY AND RADIATION CONTROL

Licensing

Early in 2000 a licence amendment to operate ISAC with a proton beam current of up to 20 μA on any target up to $Z = 82$ for a limited number of shifts per month was obtained from the Canadian Nuclear Safety Commission (CNSC). Application was made in October for a new licence as required by the change from the AECB to the CNSC regime. This application also requested operation of the ion beam accelerator system and proton beam on target of up to 100 μA. A positive response is expected by April, 2001.

Access Control and Radiation Monitoring

The ion beam radiation monitoring system (IBRMS) was expanded to accommodate new experiments as they came on line. The IBRMS was also extended in anticipation of the operation of the ion beam accelerator system and the high-energy experiments. The new emphasis on quality assurance for safety critical systems meant that the TRIUMF Safety Systems group participated in the specification, documentation and acceptance testing of the high-voltage interlocks for the β-NMR experimental station. Similarly, they defined and documented the access control requirements for the DTL X-ray enclosure and the high-energy experiments.

Commissioning

The installation of all shielding as initially specified was completed during 2000. As expected, the addition of the steel shielding between the target station and the pre-separator magnet completely eliminated the problem of neutrons streaming up to the TRINAT experiment level.

Some low levels of short-lived radioactive contamination were detected in the target maintenance hall after a target exchange. Extensive tests were subsequently carried out with a dummy target module to determine the air flows into or out of the target maintenance hot cell during the target transfer. It was verified that the air flow was always directed into the hot cell under all circumstances as predicted by the design. There has been no spread of contamination on any subsequent target exchange.

REMOTE HANDLING GROUP

ISAC Target Modules

A great deal of work on the construction of new ISAC target modules was performed by Remote Handling personnel.

The module assembly area in the ISAC experimental hall was revised to better suit the installation of the HEBT beam lines. Work continued on target module #2 with further revisions to the containment box and the construction of required spare parts.

Target module #3, which has been in shielded storage in the target hall since the 100 μA beam-heated target experiment, was removed from storage. The Mo target was removed and the shielding plug and containment box assembly moved to the experimental hall module assembly area for further work.

Target Hall

During the winter shutdown, three initial remote accessible module storage silos were completed and installed in the target hall. Modules from the ITW station were transferred to both the new silos and the ITE station vacuum tank during the spring shutdown as required for installation of additional perimeter shielding at both the ITE and ITW stations.

Design was completed for a spent targets storage vault to be located in the target hall. This will allow for interim storage of irradiated targets for either eventual re-use or as short-term decay storage prior to off-site disposal.

Beam Lines Servicing

The beam line at zone #5B between ITW and the pre-separator magnet was uncovered in January and rebuilt by Remote Handling with new iron and concrete shielding around a revised beam line with a new rad-hard valve and new beam profile monitor. Existing overhead shielding blocks were cored at this time to accommodate the new, taller design of the monitor. Preparations were completed for installation of the ITE beam line section, except for the actual monitor, at the same time. Both beam line sections are now fully remote serviceable for component handling.

Hot Cell Facility

Hot cell construction for the year included an improved inert-gas capping system for the Pb glass shielding windows, and a portable shielding plug for the roof access portal. The north and south cell access doors were fabricated, fitted and filled with concrete.

Handling procedures were improved with the design and fabrication of working prototype jigs for removal and replacement of the containment box access covers as well as for handling of the target module TIS component mounting tray.

The hot cell south support area is being provided with tooling, cabinets, a fume hood and more defined area safety control barriers.

During the 2000 operational year, the Nb #2 target was replaced with the Ta #1 target in June for a short running period. This was then exchanged for the first $CaZrO_3$ target in July. This target was in turn replaced by a SiC target in November. Revised handling procedures for decontamination and control have steadily improved, reducing previously encountered levels of movable contamination to minimal values and eliminating any spread of contamination within the target hall.

Remote Crane Handling System

Improvements continued on the remote crane operating console with improved controls and displays. A PC driven video switcher and pan/tilt control now allows for general target hall viewing both at the controls console and at selected internal network PCs. Operator training has now provided us with three fully qualified remote crane operators. The requisite six remote module transports for three target exchanges this year were performed as scheduled.

ION SOURCES FOR ISAC

Electron Cyclotron Resonance (ECR) Source

The design of a radiation hard 2.45 GHz ECR source is nearing completion.

It is based on the ECR source that was tested in the ion source test stand (ISTS) and the results reported in last year's Annual Report.

The vacuum chamber of the ISTS that was used so far to test ion source prototypes must be replaced during the first quarter of 2001 by a bigger one to accommodate and test the radiation hard ECR source prior to its installation into the ISAC target module.

Off-Line Ion Source (OLIS)

It was used throughout the year to: a) commission the ISAC accelerators, b) tune the beam transport lines and accelerators prior to operation with radioactive ion beams, and c) provide the low-energy experimental facility with stable beams.

A stable beam of Mg^{1+} ions was requested in year 2000. It was newly produced by direct evaporation of a high purity magnesium plate mounted within the plasma chamber of OLIS. Plasma interaction yielded enough Mg vapour to produce a stable 200 nA Mg^{1+} beam.

Charge State Booster (CSB)

In the ISAC-II facility, the accepted mass range is extended from 30 to 150 u.

ISAC-II will utilize the existing ISAC-I RFQ for low-energy acceleration. The CSB would take the singly charged radioactive beam from the mass separator and boost the charge state to be compatible with $A/q \leq 30$ for the RFQ.

One of the few known dc methods to boost the charge state of an ion is based on the electron cyclotron resonance (ECR) source principle. Such an ECR charge breeder (CSB) has been developed at the Institut des Sciences Nucleaires (ISN) in Grenoble [Sortais *et al.*, 5^{th} Int. Conf. on Radioactive Nuclear Beams (RNB-5), Divonne, France, April, 2000].

A research collaboration agreement between ISN Grenoble and TRIUMF was signed in September. The goal of the seven months' collaboration is to provide TRIUMF the know-how and the properties, from a realistic 1^+ beam, with the ISN charge state booster method using the ISN 14.5 GHz ECR source and $1^+/n^+$ test bench facility.

The essential points of this project are to measure: a) the efficiency of the $1^+/n^+$ process for ion species relevant to the ISAC experimental programs (such as Rb, Ga, Sr, Sn, Fe, Zn, Ar, Kr, Xe, etc.); b) the overall breeding time (of utmost importance for short-lived isotopes); and c) the proportion of unwanted species (stable contaminants) self generated by the CSB.

The TRIUMF computer controlled beam measurement system nears completion and it will be shipped to Grenoble in January, 2001. Installation and data-taking will be carried out until the end of March/April, 2001.

ISAC TARGETS

In 2000 the ISAC operating licence was upgraded to allow up to 20 μA p^+ beam current operation during four days per month for beam and target development purposes. Two target materials (Nb foils and Ta foils) have now been operated at 20 μA p^+ beam currents.

At the beginning of the 2000 ISAC run schedule, the Nb #2 foil target used in 1999 was reinstalled and continued to be used for rubidium beam production to Expts. 823 and 828/LTNO. ^{8}Li beams were also delivered to the ISAC β-NMR facility for commissioning purposes. The Nb #2 target was operated with $\leq$10 μA p^+ beam currents from April 20 to June 4. On May 26, 15 μA operation was achieved during the day shift and from June 3–4 the target was operated for 19 hours at the 20 μA proton current level. The production of ^{74}Rb was observed to increase threefold from 10 to 20 μA to a high of 6.1×10^3/s. There are indications to suggest that the nonlinear increase is due to radiation enhanced diffusion of Rb in the Nb matrix. Including the 1999 run period, the Nb #2 target received a total of 5914 μAh of p^+ for an integral dose of 2×10^{20} protons on target. After 117 days in place, the target was still operational when retired from service.

From June 14 to July 15, a 21.3 g/cm^2 Ta foil target (Ta #1) consisting of 512 foils of 0.025 mm thickness was irradiated to produce beams of ^{162}Yb for Expt. 801, ^{75}Ga for Expt. 863 and ^{8}Li for β-NMR polarizer commissioning. The ^{162}Yb yield was of order 10^9/s under 10 μA irradiation, two orders of magnitude higher than required by the experiment. The ^{75}Ga yield at 10 μA was 2×10^5/s with <0.04% ^{75}Rb contamination. For target development, two periods of 20 μA operation were used to measure yields of Li, Na, Al and K isotopes. The measured ^{8}Li yield was 8.9×10^7/s at 10 μA, with a nonlinear rise to 5.2×10^8/s at 20 μA. Yields of ^{9}Li, ^{11}Li, ^{26}Na and ^{38m}K also displayed nonlinear increases with proton current, while the longer-lived ^{38g}K did not. As with the previous Nb foil target, the nonlinear yield increase with proton current is consistent with a radiation enhanced diffusion effect. The Ta #1 target was in place for 31 days receiving 3519 μAh of p^+ for an integral dose of 8×10^{19} protons on target. The target remains operational.

A target of pressed pellets of $CaZrO_3$ (42.3 g/cm^2) was irradiated from July 23 to August 20 and again from October 1 to November 15. The thermal properties of the target material precluded proton beam currents greater than $\sim$3 μA. However, the target was successfully operated for 73 days receiving 1357 μAh of p^+ for an integral dose of 3×10^{19} protons. The $CaZrO_3$ material proved to be superior to the CaO targets previously used for production of light K isotopes. The K isotope yields were of the same order as with CaO, but with greatly reduced target deterioration. Yields of 1×10^7/s of ^{38m}K and 5×10^6/s of ^{37}K were provided to Expt. 715/TRINAT. The Zr component of the target material also allowed delivery of ^{79}Rb and ^{91}Rb to the LTNO facility for commissioning and for Expt. 826.

A SiC pressed pellet target (7.4 g/cm^2) was irradiated from November 24 to December 20. The target was used to produce ^{8}Li beams (2×10^7/s at 10 μA) for β-NMR facility commissioning and to determine Na yields for future accelerated beam experiments. Over 26 days the target received 2155 μAh of p^+ for an integral dose of 5×10^{19} protons. The target remains in place.

ISAC POLARIZER

The first transmission of unpolarized ^{8}Li through the ISAC polarizer had been achieved in December, 1999. The first four months of this year were spent preparing the system for the first polarized beam. This entailed bringing the Na neutralizer and He re-ionizer cells into operation, and fabricating and installing deceleration electrodes, deflection plates, magnetic coils, a fluorescence monitor, laser beam polarization and transport systems, associated safety equipment and controls. The argon ion laser and Ti:sapphire laser used to collinearly pump the ^{8}Li beam were borrowed from the I4 polarized H^- ion source. The Ti:sapphire laser cavity mirrors had been customized to allow lasing at 673 nm, giving us a rudimentary polarization system.

A brief test in May produced 10–15% polarization, estimated from β-decay asymmetries. This was an encouraging result, considering that the laser parameters were far from ideal for collinear optical pumping. The standing-wave laser had a time-averaged bandwidth of approximately 2 GHz (FWHM) and lased chaotically on about 20 cavity modes with 700 mW total power. (The ideal laser should lase simultaneously on two modes separated by the 381 MHz Doppler-shifted hyperfine splitting in the ^{8}Li ground state.) The test also showed that the D_1- and D_2-transition fluorescence monitor, used for tuning the ^{8}Li beam energy into resonance with the laser, had a signal to noise ratio of about 15 at the estimated ^{8}Li current of 10^7 atoms per second. Polarized $^8Li^+$ transmission efficiency through the polarizer was 60%.

The laser was modified for the next β-NMR run, July 4–12. The laser cavity length was shortened to increase the cavity mode spacing from 220 MHz to 358 MHz ($\pm$1 MHz) and the free spectral range of the uncoated intra-cavity tuning etalon was decreased from 200 GHz to 100 GHz. (All laser cavity mode spacings were only known accurately in retrospect, following the implementation of an accurate beat measuring technique in January, 2001). This had the intended effect of reducing the number of lasing cavity modes (by a factor of 3) while leaving the total power unaffected. The highest ^{8}Li polarization observed was about 40%. In addition, polarization could be kept at 30–35% for several hours by non-specialists, using an automated stabilization system, and re-tuned by non-specialists when the polarization dropped. The stabilization system was based on a laser spectrum analyzer locked by computer to a frequency stabilized HeNe laser. The drift of the Ti:sapphire laser was monitored by computer with the spectrum analyzer, and compensating changes were made to the Na cell bias to keep the ^{8}Li beam energy in resonance with the laser. The hyperfine splitting was resolved by the fluorescence monitor, with a signal to noise ratio of about 50.

The final β-NMR run this year was $3\frac{1}{2}$ weeks in November and December. During the July run, the laser still hopped chaotically between modes. Therefore many ^{8}Li atoms, traversing the polarizer in 2 μs – much less than the mode-hopping time – did not see the laser light, or saw only one mode. Further modifications to the laser between July and November involved increasing the mode spacing to 368 MHz, and increasing the etalon finesse by coating both surfaces with 10% reflectivity layers. This finally made it possible to produce simultaneous lasing on only 2 modes, with a total power of about 200 mW. (Note that the power per mode did not drop.) However, despite this improvement, the measured ^{8}Li polarization dropped by half compared to July, for reasons not understood. Progress on diagnosing the problem was hampered by the very low beam intensities available – approximately 10^6 atoms/s at the start of the run, dropping to 10^5 atoms/s when the polarized ion source I4 was brought into operation. In the latter case, it was not possible to obtain a useful fluorescence signal, although tuning was possible using the β-NMR asymmetry signal.

By year end, we were ready to upgrade the Ti:sapphire laser to a perfect 381 MHz spacing between just 2 cavity modes, with no drift in laser frequencies. This is achieved by placing one of the laser mirrors on a piezo-electric mount, which allows active stabilization of the cavity length using the laser spectrum analyzer as a monitor. In addition, in December a used ring dye laser arrived on site on indefinite loan from KEK, Japan. The plan is to have the ring laser set up for the next β-NMR run. A single frequency ring laser can be used as a more conventional, albeit expensive, method of polarizing ^{8}Li and it is also a precise diagnostic tool. It is also essential for polarizing ^{7}Li, which is useful for stable beam tests, and for polarizing ^{11}Li, an isotope required for a recently approved experiment.

ENGINEERING

Engineering support is initiated by the submission of a Request for Engineering Assistance (REA) form. These are assessed, assigned, and reviewed weekly. During this report period there were 35 ISAC REAs submitted. 12–15 others were carried over from the previous year as large projects, several of which will be carried over to 2001, i.e., DRAGON and target modules (TM2 and 3).

The following is a brief description of some of the major tasks that Engineering participated in during this period.

- Target modules: TM3 had been completed far enough to allow its use in a 100 μA non-RIB test in December, 1999, and then it was stored in the target hall. TM2 was built during 2000 and will be completed in the spring of 2001 as a surface ion source module. TM3 will be completed in 2001 as an ECR source (availability sometime in 2002).
- East target station: An REA was submitted and a budget approved to design and build an entrance and dump module for the east target station. This did not occur due to lack of manpower and priority, but will definitely reappear in 2001.
- Conditioning station: An REA for this job first appeared in early 1999, but work did not commence until 2000. The conditioning box and stand were manufactured and are currently awaiting assembly. The remainder of the station (i.e., beam line and diagnostics) have yet to be completed, but completion of the box would still allow for target conditioning.
- ECR source: This is another carry-over project that has been through many design iterations due to mechanical/manufacturing considerations, as well as information from development work. Release to manufacture is imminent.
- DTL: The year 2000 saw the completion of tanks 2 through 5. The tanks, stands, ridges and stems were put out for tender and manufactured by local industry. Assembly was completed at TRIUMF, and installation and alignment achieved later in the year. This also involved design and manufacture of four triplet magnets associated with tanks 2 through 5. Successful stable beam transmission was accomplished just before Christmas.
- HEBT buncher: A 35 MHz spiral buncher was designed, detailed and manufactured. This buncher was a larger version of the MEBT buncher and will be installed and commissioned in 2001.
- Remote handling issues: There were a series of engineering meetings held to discuss remote handling issues unique to ISAC (in the target hall and hot cells). This is of primary importance in order to develop procedures that allow for successful RIB production and target changes in a safe way that ensures contamination control. These meetings were a forum for exploring options for such things as hot target storage, contamination control, decontamination of components requiring maintenance, north hot cell configuration, south hot cell completion (i.e., doors and turntable), hot cell procedures and fixtures (i.e., tray removal), and priorities and schedule. Examples of some actions are as follows:
  - Hot cells: The drive for the hot cell turntable was redesigned to deal with a higher rotational resistance than expected. This will be installed in 2001. Shielding doors to both cells were designed and built during this period and will be installed in early 2001.

– Decontamination station: There is a requirement to have a place within the target hall to work on components from the target station, vacuum system components, diagnostic equipment, etc., that have become active and contaminated. To this end it was decided to investigate ways and means of decontaminating these components. This work was undertaken by an engineering summer student who designed and began construction of a prototype test station involving pressure washing, ultrasonic cleaning, and electrocleaning. This work is still under way with tests planned in the new year (a preliminary report is available on this work).
– Hot cell fixtures: At the beginning of this report period the south hot cell was limited to changing targets. It was soon recognized that problems with the extraction column of the target module tray or optics/diagnostics on the exit module tray probably would not be able to be repaired without removing the tray and replacing it. To this end a fixture was designed and built to do this within the hot cell. This is only a beginning and no doubt will require refinement once tested. There are many other tasks and procedures that also need to be addressed in the near future to make the cells fully operational.

- DB0: This is the diagnostic station downstream of the pre-separator magnet. It houses slits, a profile monitor and a Faraday cup. The slits become active and contaminated during operation, making maintenance of any part of the diagnostic box very difficult. Engineering provided assistance to the Probes group in redesigning the box so that the slits could be removed and stored in a pig prior to servicing. This new diagnostic box will be installed in early 2001.
- Spare components: In order to provide replacement trays for the target and exit modules, an order for spare components was put in the Machine Shop early in the year. These spares have been received and sorted. However, at the present time manpower is lacking for assembly.
- ISAC-II: An REA was submitted to provide engineering support for the superconducting prototype rf cavity currently under construction in Italy. This support so far has concentrated on a study to look at alternative cavity tuners. In-parallel engineering assistance was provided to design and build a test cryostat which has been sub-contracted to Quantum Technologies. TRIUMF will design and build a copper cavity dimensionally similar to the niobium cavity to allow for prototype testing.
- DRAGON: Engineering support for the DRAGON project continued throughout 2000, with two personnel almost full-time. A full report of the activities can be found in the Mechanical Engineering subsection of the Accelerator Technology Division section.
- Target hall tasks: Engineering, along with Operations and Remote Handling, produced a list of outstanding issues related to the target hall. These were presented and discussed at several engineering meetings. They fall under the headings of modules, target hall, ion source, and hot cell. This was done to try to identify and consolidate unfinished tasks, tasks not started, and tasks without a solution. It is hoped that this listing will provide a platform to investigate and optimize priorities, schedule and manpower for the coming year.

RF SYSTEMS

RFQ

The RFQ operated very reliably for the various stages of this year's beam commissioning tests. The only attention required was the occasional high power pulsing to reduce the buildup of dark currents.

MEBT

Bunch rotator

The triple gap split ring assembly for the bunch rotator was developed and fabricated at INR RAS, Russia. The effective voltage is 60 kV at a power level of 3 kW. The tank, originally fabricated for the prototype DTL buncher, was modified to accept the bunch rotator structure. Signal level tests confirmed the design parameters and the cavity is now ready for power tests.

Choppers

In order to meet all the demands for chopping, a system of two sets of plates at 5.9 MHz and 11.8 MHz, capable of being dc biased, was adopted. Figure 133 shows a 3D view of the dual frequency chopper.

The chopper design was completed and the fabrication started. One of the critical components of the chopper is an rf feedthrough at 7.4 kV. This was developed in-house since it was not available commercially. The feedthroughs are attached to the top plates for rf voltage, and the capacitors attached to the bottom plates are for dc bias.

Rebuncher

The 35 MHz rebuncher was commissioned this year and operated reliably for beam commissioning tests.

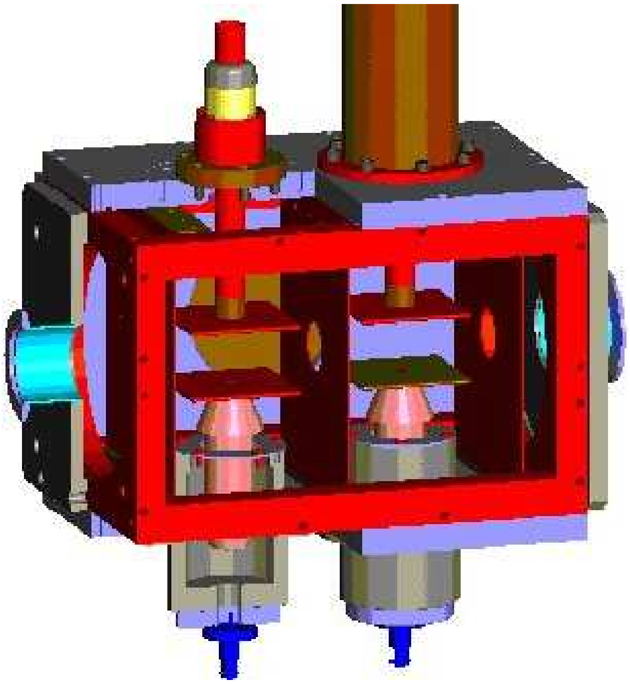

Fig. 133. 3D view of the dual frequency chopper.

DTL

The variable energy DTL is based on five independent interdigital H-type (IH) structures operating at 106 MHz. The first four tanks have been tested to full power in the test facility and are installed in the ISAC accelerating complex. Tank 5 was installed in the ISAC accelerating complex with only signal level tests performed, but has operated at half power for beam tests.

The variable energy DTL also requires three independent 106 MHz bunchers operating at low beta of 2.3%, 2.7% and 3.3% respectively. These bunchers are triple gap split ring resonators, which were developed and constructed at INR RAS, Russia and tested at TRIUMF. All three bunchers have been tested to full power in the test facility and are now installed in the ISAC accelerator complex.

Figure 134 shows the tanks and bunchers installed in the ISAC accelerator complex. All eight DTL power amplifiers have now been successfully tested into a resistive load. Five of these amplifiers have operated at half power into the five DTL tanks.

IH tanks

Following the assembly and mechanical alignment of the DTL tanks, signal level measurements were carried out. Figure 135 shows the tanks in various stages of assembly and test.

The resonant frequencies of the tanks range from 0.4% to 1.3% higher than the operating frequency. All the tanks are equipped with adjustable coarse tuners to

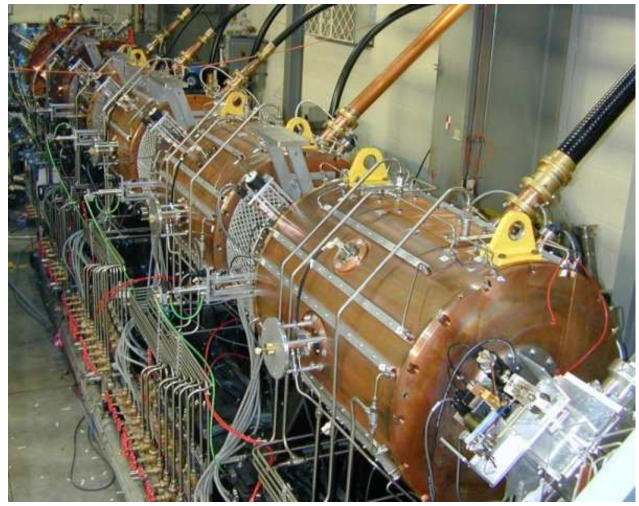

Fig. 134. DTL tanks and bunchers installed in the accelerator complex.

Fig. 135. DTL tanks in the assembly area.

bring the resonant frequencies within the tuning range of the fine tuners. The coarse tuners have a tuning range of 500 kHz, whereas the tuning range of the fine tuners is only 100 kHz. Bead pull measurements were performed on all the cavities to determine the field distribution along the drift tubes and to estimate the shunt impedance of each DTL. The field distribution agreed with the MAFIA predictions. The field distribution in tank 2 showed a slight tilt to the field along the axis, but the field variation was within $\pm 2\%$. The field distribution in the remaining tanks was more typical with no evidence of a tilt. Both the shunt impedance and Q obtained from measurements are lower than values predicted from MAFIA, leading to higher power requirement from the power amplifiers. Except for the loop size, the same rf power couplers have been used in all the structures. From measured shunt impedances, the power required to attain designed peak effective voltages of 1.18 MV, 1.96 MV, 2.15 MV and 2.2 MV for DTL tanks 2, 3, 4 and 5 respectively were calculated to be 10.0, 16.0, 19.0 and 21 kW.

When tank 2 was first powered up it became evident that we would have to add some cooling to the tank walls, even though MAFIA calculations indicated otherwise. For a quick fix, it was decided to clamp on a $\frac{1}{2}$ in. square copper cooling line with strips of indium between the cooling line and the tank wall for improved thermal conduction. This kept the outside temperature of the tank below 50 degrees for full power operation. The same solution was used for tank 3, but a further investigation was carried out with different thermal conducting compounds for a more permanent solution for tanks 4 and 5 which operate at a higher power level.

A coupon of steel material was used to simulate a section of the tank wall and a length of square copper cooling line was attached to the coupon using different materials. The coupon was heated using a normal kitchen hot plate. Thermocouples were used to keep the power somewhat constant and to measure the thermal gradient across the interface of the cooling line and the tank. The results are shown in Fig. 136 normalized to Certanium solder. Since these measurements were not done in a controlled environment there is probably a large error bar, but the evidence was strong enough to indicate that the CHEMAX compound was better than indium. The other compounds which were tested, although they showed similar thermal characteristics to CHEMAX, are pastes and very messy to deal with; whereas CHEMAX is a curing compound. With the cooling problem solved, the tanks were tested at power.

DTL tanks 2, 3 and 4 were tested to full power of 10 kW, 16 kW and 20 kW respectively in the test stand. During the power test, it became evident that the fine tuner cooling also had to be improved. The initial design had a water-cooled heat sink at the extreme end of the tuner shaft. This was replaced by a design that water-cooled the shaft all the way to the tuner plate.

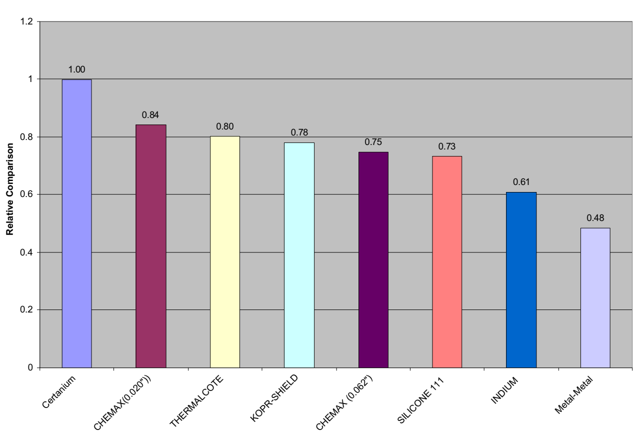

Fig. 136. Thermal conduction graph.

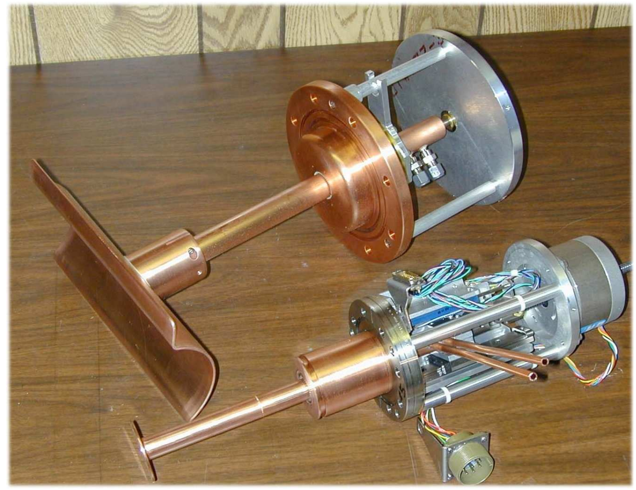

Fig. 137. DTL tank fine and coarse tuners.

The fine tuner along with the coarse tuner are shown in Fig. 137. The tanks were baked with hot water at 60°C for 6 to 8 hours to reduce the conditioning time and the time to get through multipacting. The power tests were performed inside a shielded bunker and X-ray emissions were monitored to meet the personnel safety requirements. X-rays emitted from the tanks were measured and compared with drift tube voltages estimated from input power and measured shunt impedances.

Triple gap bunchers

The rf parameters, resonant frequency, Q, shunt impedance and field distribution of the three bunchers have been determined from signal level and bead pull measurements. The bead pull measurements show that the difference between two end gaps is within ±1.8% to ±4.6% for the three bunchers. Because of the construction of the split rings, it is difficult to obtain better accuracy than this. The nominal power required for bunchers 1, 2 and 3 is 8 kW, 10.2 kW and 11.6 kW to obtain the designed peak effective voltages of 190 kV, 260 kV and 320 kV, respectively. The bunchers are equipped with fine tuners, which have a tuning range between 200 and 500 kHz. One of the bunchers is shown in Fig. 138.

The bunchers have been successfully tested to full power in the test facility. Drift tube gap voltages were measured with X-ray field emissions and compared with voltages estimated from input power and measured shunt impedances. Excellent agreement between these measurements was obtained.

HEBT

Low beta buncher

The 11.9 MHz low beta (2.2%) prototype buncher was completed and is shown in Fig. 139.

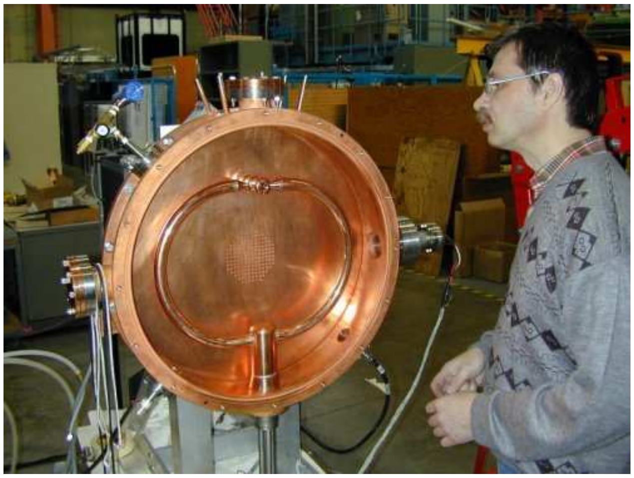

Fig. 138. One of three DTL bunchers.

Fig. 139. The 11.9 MHz buncher prototype.

One of the critical components of the buncher is the rf feedthrough at 30 kV shown in Fig. 140. This was successfully developed and tested in-house since it was not available commercially. The design of the three-gap structure has started. The buncher requires two rf feedthroughs, two fine tuners and two resonant tank circuits driven from a single 2 kW power amplifier.

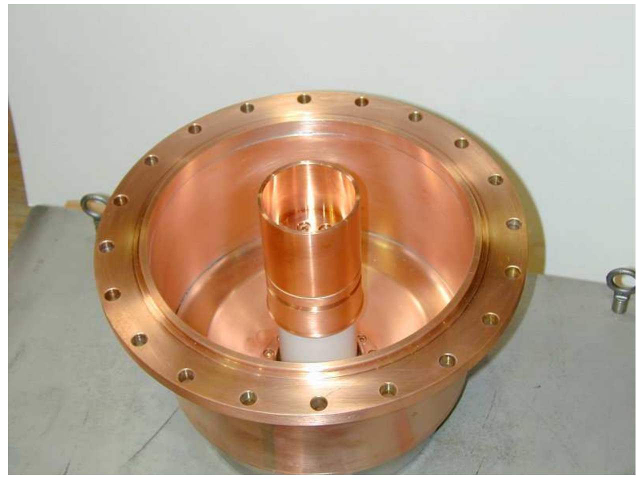

Fig. 140. Feedthrough for the 11.9 MHz buncher.

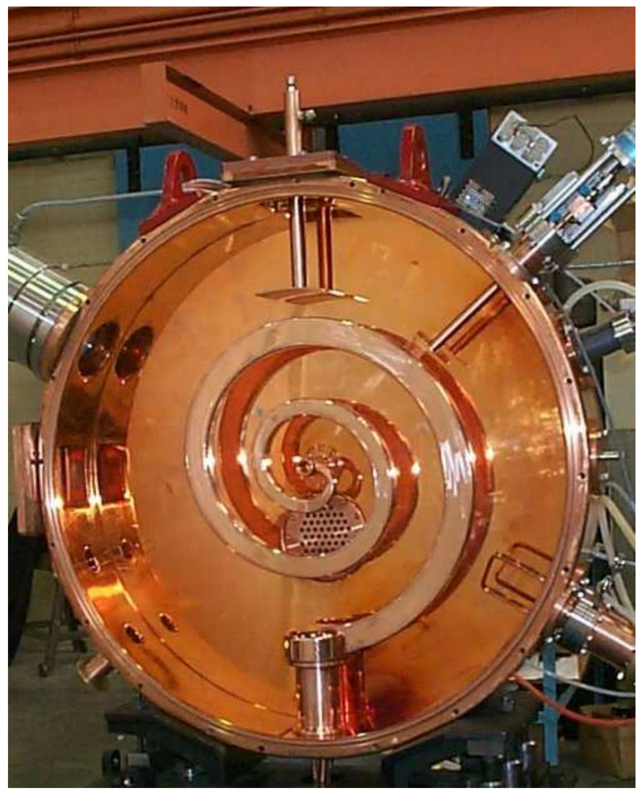

Fig. 141. The 35 MHz high beta buncher.

High beta buncher

The 35 MHz high beta (3.2%) buncher was fabricated and assembled and is shown in Fig. 141 with the tuners and coupling loop installed, ready for signal level tests.

The measured resonant frequency and Q of the buncher's two-gap cavity are within 1% and 70% of the values predicted by MAFIA 3D simulation, respectively. From the bead pull measurement the estimated power required to produce a peak effective voltage of

270 kV is 12 kW, and the field error was measured to be ±1.7%. Realigning the drift tube more precisely will further reduce the field error.

Due to a buildup of copper during the plating process, the tank edges are being re-machined and re-copper plated to provide better contact between the tank and the copper end plates. At the same time, cooling channels on the tank outer surface are being machined for the installation of water cooling lines. Following re-installation of the coarse tuner, fine tuner and coupling loop, plus precise re-alignment of the drift tube, signal level measurements will be completed before power tests can begin.

RF Controls

The RF Controls group has commissioned the entire rf structure between the MEBT and the HEBT. This includes 5 DTLs, 4 bunchers, and 1 rebuncher. The control systems for these rf structures are housed in 3 separate VXI mainframes located in the mezzanine area. Each of these structures has three separate feedback regulating loops, controlling the in-phase and the quadrature-phase control of the rf voltages, and the tuning of each rf cavity. These feedback control loops utilize digital signal processors to achieve high degrees of stability and flexibility. The stability aspect is demonstrated in achieving rf voltage regulation with amplitude error less than 0.1% and phase error less than 1°. The flexibility aspects are demonstrated in using the same design for all the rf structures, and we were able to condition and to commission all rf structures in a very short time.

ISAC ACCELERATOR COMMISSIONING

The ISAC accelerator is being commissioned in stages. The RFQ was commissioned in two stages: an initial 7 ring configuration was tested with beam in October, 1998 and the final 19 ring configuration was tested with beam in September, 1999. For historical reasons, the 19 ring test to the stripper foil box of MEBT was termed Test #1. This year Test #2 and Test #3 were completed and Test #4 was initiated. Test #2 involved beam tests with the stripping foil and the commissioning of the MEBT charge selection section, while Test #3 involved the installation and commissioning of the last section of MEBT and the first subsection of the DTL consisting of the first tank, tank 1, the first triplet, triplet 1, and the first INR buncher, buncher 1. Test #4 concerns the commissioning of the full installation of the DTL and first section of HEBT.

Test #2

In Test #2 a diagnostic station consisting of a profile monitor, a Faraday cup, a fast Faraday cup, and a transverse emittance rig were positioned downstream of the MEBT charge selection section. The test was designed primarily to observe the effects of the stripping foil on the beam and to commission the MEBT charge selection section. Beams of $^4He^{1+,2+}$, $^{14}N^{2+,3+,4+,5+}$, and $^{20}Ne^{4+,5+,6+}$ were used in the beam test. The profile monitor at the image point of the charge selection section was used to establish an achromatic tune through the charge selection section. The emittance rig was used to study the emittance growth of the beam through stripping and through the effects of foil aging. The data from the transverse emittance study are summarized in Table XXIII. An emittance rig located just before the RFQ is used to measure initial beam emittances. Emittance measurements for the helium beam are given in Fig. 142. The He beam is interesting in that it is not necessary to strip the beam to bend it in MEBT, so both stripped and unstripped data were taken.

Table XXIII. Normalized transverse emittance values measured before and after stripping for various beams and charge states.

Beam	E	Q	Strip	$\beta\epsilon_x$	$\beta\epsilon_y$
	(keV/u)			(mm-mrad)	(mm-mrad)
^{4}He	2	1	×	0.028π	0.027π
	153	1	×	0.048π	0.050π
	153	1	√	0.083π	0.081π
	153	2	√	0.083π	0.080π
^{14}N	2	1	×	0.031π	0.038π
	153	3	√	0.096π	0.096π
	153	4	√	0.100π	0.096π
	153	5	√	0.093π	0.096π
^{20}Ne	2	1	×	0.017π	0.016π
	153	4	√	0.052π	0.059π
	153	5	√	0.052π	0.057π
	153	6	√	0.048π	0.055π

The effect of energy straggling on the energy spread and energy of the beam were investigated both at the symmetry plane of the charge selection section where there is a dispersed focus, and at the fast Faraday cup (FFC) in the diagnostic station. Comparisons of the symmetry plane beam spot for stripped and unstripped He beams showed both an increased energy spread and energy drift due to energy straggling. The TOF of the beam to the FFC gradually increased as the stripper aged, indicative of foil thickening. The foil was observed to develop a small blackening corresponding to the irradiated spot. Mass spectra of the stripper foil box indicated oil contamination in the vacuum. It is postulated that the oil molecules crack on the foil during bombardment and progressively thicken the target. Eventually the thickened spot overheats and a rupture occurs in the foil. An illustration of the foil aging is given in Fig. 143. Here a neon beam is observed at

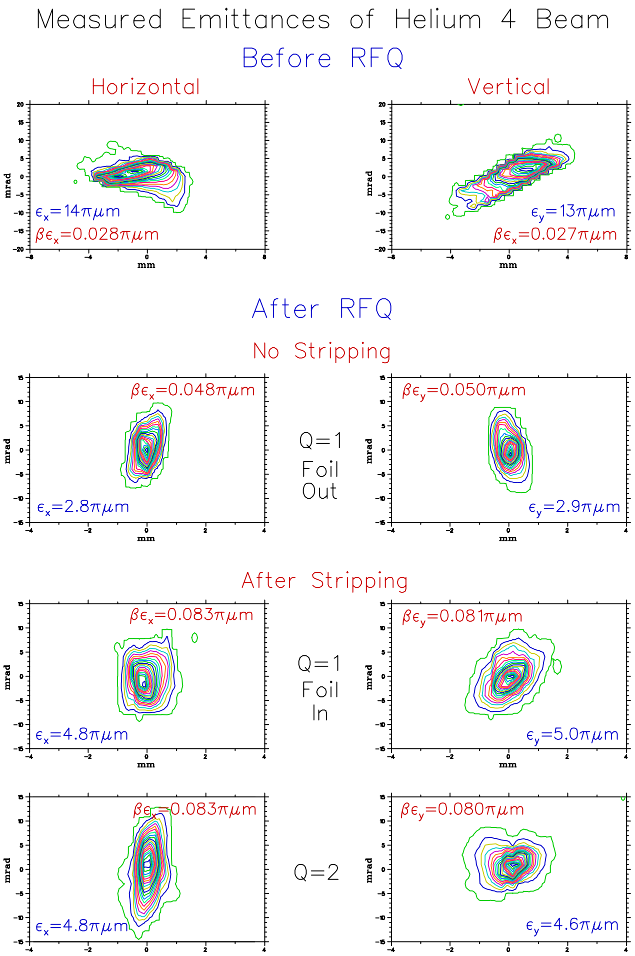

Fig. 142. Transverse emittance measurements for a He beam; both stripped and unstripped values are given, as well as the emittance before the RFQ.

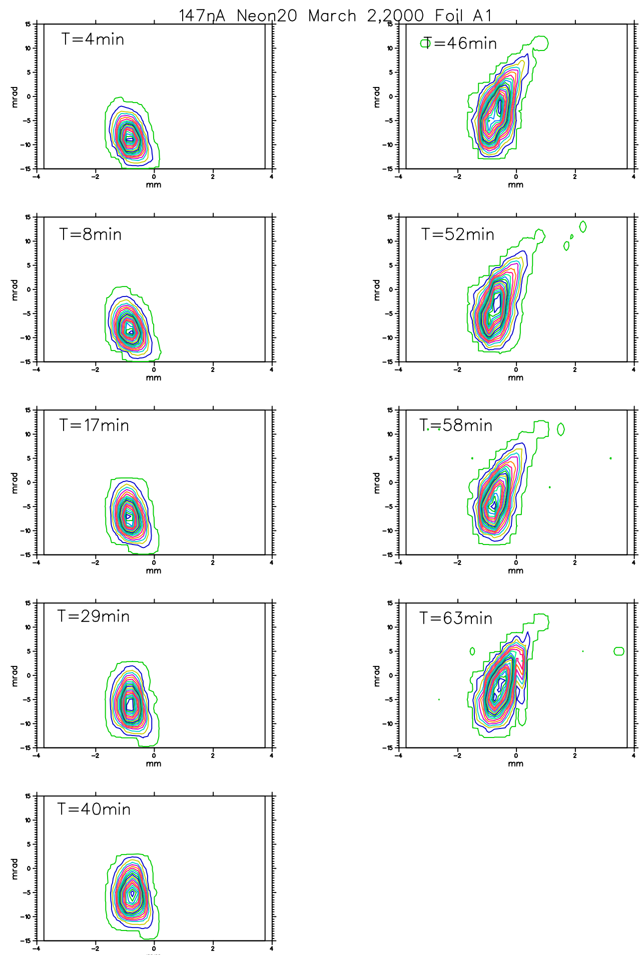

Fig. 143. Transverse emittance measurements for a Ne beam showing foil degradation over time.

the emittance rig over time in transverse phase space. Since the bend is only singly achromatic, as the foil thickens the beam slows and drifts to more positive transverse momentum and a tail develops before the foil eventually disintegrates at ∼60 minutes. Foil lifetimes shortened as beam mass increased. Foils lasted indefinitely for He beams, while with Ne beams useful foil lifetimes were in the range of 50 nAh. Although most radioactive beams will be of low intensity, the lifetime is a concern especially during stable beam operation. We plan to reduce the buildup by cleaning the section, adding a cold trap around the stripping foil and, if required, provide a beam feedback signal to a bias voltage on the stripping foil to correct for the energy loss.

Test #3

For this test the first complete subsection of the DTL consisting of the first IH tank, tank 1, plus a quadrupole triplet, triplet 1, and triple gap buncher, buncher 1, was installed. The test allows us to perform rf conditioning *in situ*, debug rf controls, establish alignment procedures, commission the injection line and triplet, determine matching conditions, and measure beam quality all well in advance of the final installation.

Beam dynamics

At full voltage the beam dynamics are typical of a 0° accelerating structure; matched beams enter each accelerating section converging in all dimensions and after acceleration the now diverging beams are refocused before the next accelerating section.

At a reduced tank voltage the particle bunch is phased negatively with respect to the synchronous phase, so that as the particles lose step with the synchronous particle and drift to more positive phases they gain the required energy. The upstream buncher is used to match the beam to the de-tuned tank. The buncher following the tank is then used to capture the diverging beam. In Fig. 144 we show the initial and final position of a grid of particles in longitudinal phase

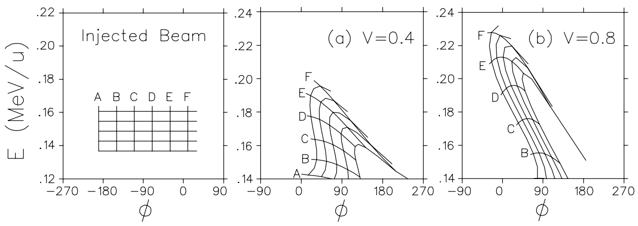

Fig. 144. Final position in $E - \phi$ space of an initial grid of particles after acceleration through tank 1 for relative voltages of 0.4 and 0.8 with respect to the full energy case.

space after simulated acceleration in tank 1 for two different relative tank voltages, $V/V_o = 0.4$ and 0.8. Distortion of phase space occurs for phases near 0°. Below this the energy gain falls off nearly linearly with phase.

Test set-up

A schematic of the test set-up is shown in Fig. 145. The medium energy beam transport (MEBT) transports the beam between the RFQ and the DTL. The MEBT consists of a matching section for the stripping foil, a charge selection section, and a final matching section before the DTL. This matching section includes a 35.4 MHz spiral buncher and four quadrupoles. Narrow diagnostic boxes upstream of both the MEBT rebuncher and DTL-tank 1 each house a profile monitor (x, y) and Faraday cup (FC).

Tank 1 consists of 9 cells covering a velocity range from 0.018 c to 0.022 c, with a maximum effective voltage of 0.5 MV, yielding a maximum final energy of 0.24 MeV/u for $A/q = 6$ and a length of 26 cm. The first split ring buncher has a design velocity of 0.023 c, a maximum effective voltage of 0.19 MV and a length of 10 cm. The diagnostic station downstream of the tank 1, triplet 1 and DTL-buncher 1 includes Faraday cups (FC) for beam transmission measurements, a slit and harp transverse emittance rig, two fast Faraday cups (FFC) for pulse width and TOF measurements, and a 90° bending magnet with a dispersion of 3 cm/%$(\frac{\Delta p}{p})$ to analyze the energy and energy spread of the beam.

Beam tests

Test results reported here are for unstripped beams of $^4He^{1+}$ (300 nA) and beams of $^{14}N^{4+}$ (100 nA) stripped with a 3–5 μg carbon foil. These ions require moderate DTL voltages. In a separate test, the successful acceleration of $^{14}N^{2+}$ proves operation at high rf power ($A/q = 7$). Unfortunately the MEBT dipole's upper field strength is not sufficient to capture all the beam from the RFQ for this ion. In all cases 100% transmission through the DTL is achieved.

The transverse emittances injected into the DTL are typically 0.06 $\pi\mu$m. The longitudinal emittance is measured by varying the MEBT rebuncher while measuring beam energy spread and pulse width, and gives a longitudinal emittance (95% included) of 0.6 π keV/u-ns for the unstripped beam and about two to three times this for the stripped beam. Long term stability of a tune was hampered by foil aging; carbon buildup on the foils caused a gradual reduction of beam energy and thus drift in the beam phase. Typical beam intensities of 100 nA of nitrogen resulted in foil lifetimes of 1–2 hours.

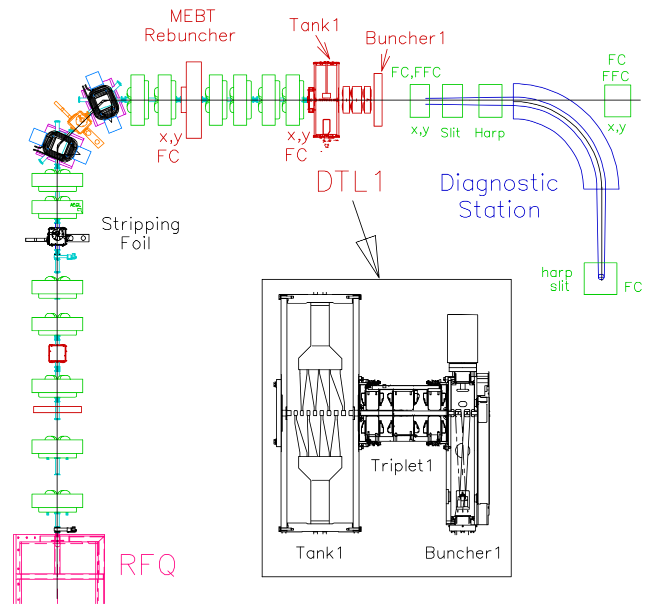

Fig. 145. Test #3 set-up.

Energy variation

Beam energy and pulse width measurements for various tank 1 voltage and phase values (buncher 1 off) confirm that variable energy operation works as predicted. Measured energy spectra for a relative tank voltage of 72% and at various rf phase set-points are given in Fig. 146(a). For each setting the MEBT rebuncher voltage was optimized to produce the best longitudinal beam quality. In general there are a broad range of voltage settings available to achieve a given energy, while still maintaining acceptable longitudinal beam characteristics. For a fixed energy, a lower tank 1 voltage (more positive phase) requires a stronger MEBT rebuncher setting for best beam quality. Measured tank 1 voltage and phase values to achieve a given energy are plotted as solid contours in Fig. 146(b) and compared to simulation results (dashed lines through large open squares). Agreement is good except at the high voltage/low phase regime where some discrepancy exists that requires further investigation.

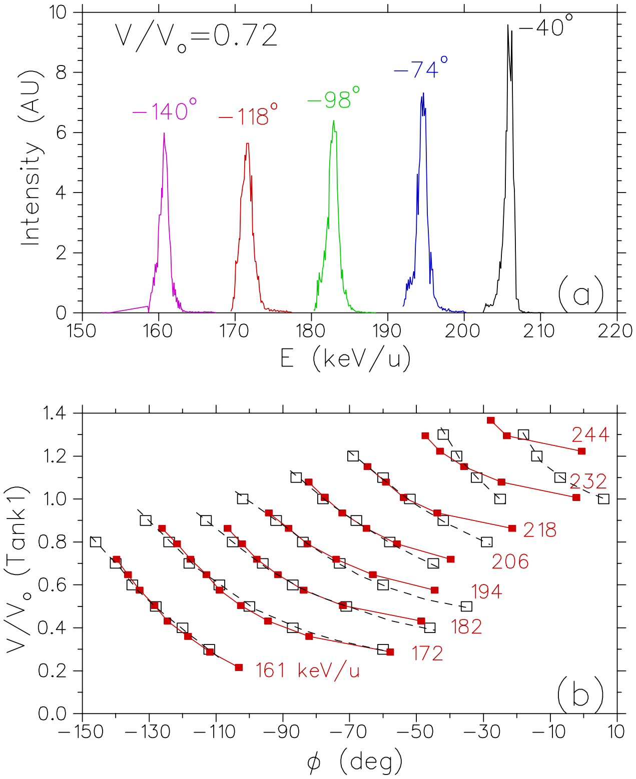

Fig. 146. In (a) the tank 1 voltage setting is fixed to $V/V_o = 0.72$ and the phase altered to produce various energy spectra for $^4He^{1+}$. In (b) a summary plot shows the resultant final energy contours as a function of tank 1 voltage and phase; the small filled squares (solid lines) correspond to measured values and the large open squares (dashed lines) correspond to simulated values.

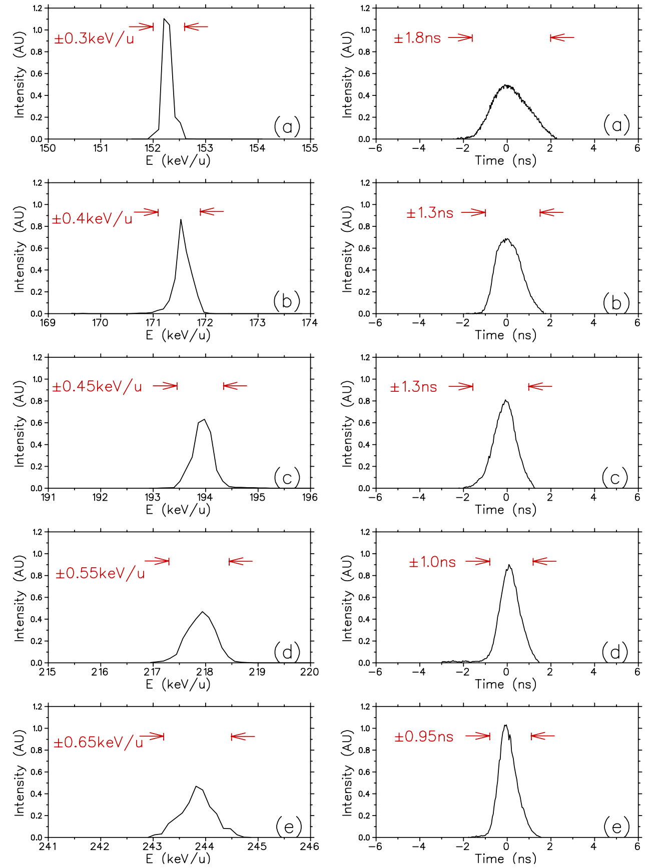

Fig. 147. Beam results giving final energy spectra and pulse width for five sample energies covering the full accelerating range of the first DTL subsection.

Longitudinal emittance

Longitudinal emittance measurements of the accelerated beam are done by varying the buncher 1 voltage and measuring the energy and time spectra at an energy spread minimum. Sample spectra are given in Fig. 147 for the $^4He^{1+}$ beam. These spectra give emittance values of 0.5–0.6 π keV/u-ns, consistent with little or no longitudinal emittance growth over the whole energy range.

Transverse emittance

Transverse emittance measurements for the $^{14}N^{4+}$ beam are summarized in Fig. 148. Shown are phase space densities and computed normalized emittances (4RMS values) before the RFQ, after RFQ acceleration and stripping, after rebunching in MEBT, after acceleration to full energy in tank 1, and finally after rebunching in buncher 1. The largest emittance increase occurs in the stripping foil, with only a small increase during acceleration. This could be improved after the planned installation of another profile diagnostic downstream of buncher 1 to further control beam size during acceleration. Emittance measurements at two lower energies, 200 keV/u and 215 keV/u, give final transverse emittances consistent with those at 230 keV/u (Table XXIV).

Table XXIV. Measured emittances of a $^{14}N^{4+}$ beam for different cases.

Description	E (keV/u)	$\beta\epsilon_x$ (mm-mrad)	$\beta\epsilon_y$ (mm-mrad)
LEBT	2	0.021π	0.021π
After stripping	153	0.059π	0.072π
After MEBT35	153	0.068π	0.074π
After tank 1	200	0.084π	0.082π
After tank 1	215	0.081π	0.078π
After tank 1	231	0.077π	0.075π
After INR1	231	0.077π	0.088π

Test #3 demonstrated the versatility of the separated function concept. New tunes were established in a short time and the measured beam quality matched predictions of beam simulations. As well, the test helped to identify potential future problems. Initial difficulties with phase-locking all rf devices due to the limited RFQ tuner range and microphonics in buncher 1 were eventually overcome. Foil thickening was

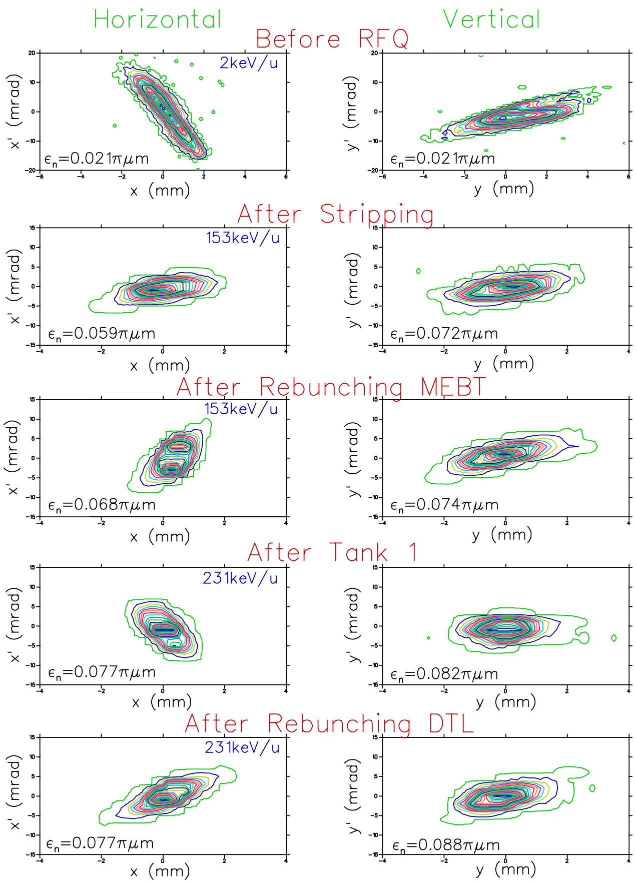

Fig. 148. Transverse emittance measurements after various stages in the beam test.

identified as being responsible for beam phase shifts in the DTL.

Test #4

The latest test (still in progress), Test #4, involves beam tests of the full DTL installation through to the first section of HEBT up to and including the HEBT beam diagnostic station. The assembly, pre-testing, installation and alignment of DTL and HEBT components was a monumental effort and resulted in the first beam being accelerated to the full ISAC design energy of 1.5 MeV/u on December 21. A first spectrum of the full energy beam from the DTL is shown in Fig. 149.

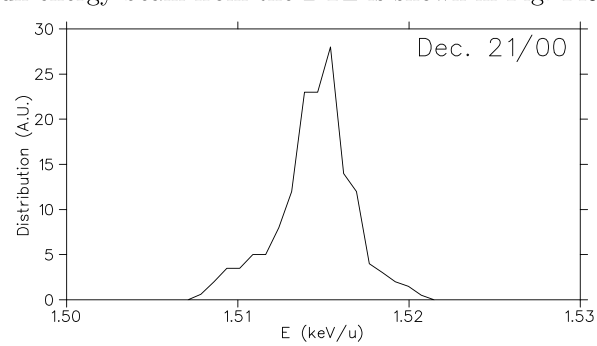

Fig. 149. First full energy beam spectra from ISAC DTL.

ISAC CONTROLS

Detailed design and implementation of additional sections for the ISAC control system again proceeded smoothly and the following major milestones were achieved.

- February: Vacuum, optics and diagnostics control for part of the MEBT beam line for Test #2.
- June: Vacuum, optics and diagnostics additions to MEBT beam line for Test #3.
- July: Upgrades to β-NMR beam line including laser control and stabilization.
- July: Vacuum system control for DRAGON gas target.
- December: Vacuum, optics and diagnostics control for DTL and HEBT into the Prague magnet.

During the year, controls for 380 new devices were added to the ISAC control system for a total of 1330 devices.

In September, Sergei Kadantsev left the group for the greener pastures of local industry. He was replaced by Evgeny Tikhomolov in December. During shutdown periods, Chris Payne from ISAC Operations was a valuable addition to the Controls group.

Hardware

Three new VME crates were added to the control system for the EPICS IOCs for DTL, HEBT, and DRAGON.

Control of the MEBT optics devices was moved from the off-line source IOC to the DTL IOC, where an additional network loop was installed with the CAN-bus controllers for the DTL and HEBT power supplies. Polarity control for the MEBT, DTL, and HEBT steering magnets was initially implemented with VME I/O modules and proved to be inefficient both from software and installation points of view. Therefore new CAN-controller adapter cards were developed, which drive the relays and contactors of the power supply load switches. For the ILE2 polarizer laser system, special CAN controllers were installed for the bi-refringent filter, etalon, spectrum analyzer bias, and cavity length stabilization.

A breakout cabinet for the diagnostics signals in the MEBT and DTL sections was installed. Due to the step-wise installation for Tests #2, #3 and #4, this panel had to be re-wired several times in the field and turned into a major labour sink. All diagnostics devices in these sections were connected and tested. Relays were installed in all rf amplifiers for remote on/off/reset control.

Three more PLC breakout cabinets were built, prewired and installed for the vacuum systems of DTL, HEBT, and the DRAGON beam line. All vacuum devices for MEBT, DTL, HEBT, the β-NMR and TUDA experiments, and the DRAGON gas target were connected and commissioned. A fourth MODICON PLC and additional Modbus segments were installed for servicing the west target station including the mass separator. This was necessary in order to decouple the target operation and the ongoing development work for the ILE1 and ILE2 beam lines.

Software

PLC ladder logic programs were written for the vacuum systems of DTL, HEBT, TUDA, the DRAGON gas target and the DRAGON beam line. The section for the β-NMR was modified to support the final beam line layout. During a two-week target change in June, the PLC ladder program for the target, mass separator and low-energy beam line sections was split and moved into two separate PLCs. This non-trivial operation was very successful and significantly simplified the commissioning of downstream systems.

ISAC standard EPICS display pages and supporting scripts were created for all subsystems. Device control panels for all new optics and diagnostics devices were created using the edd display editor. Device control panels for new vacuum devices were generated by Perl scripts. Initially, the interlock display on the vacuum device panels was generated from the interlock specification database. This led to a few confusing situations when the specification database was out of synch with the PLC program. Therefore a program was written which uses the PLC program as master for the interlock panel generation.

The EPICS display manager program was modified to allow saving and restoring of console window configurations. Also, a subtle bug was corrected which had caused annoying program crashes. These changes were fed back to the EPICS collaboration.

The parameter save/restore system was upgraded to be sensitive to the selected beam delivery modes of both the target ion source and the off-line source. In addition, a script for selective restoring of machine parameters with tolerance checking was written.

Because of the mixed experience with the available data archiving tools, a new data archiver was written. It collects data via EPICS monitors and archives to ASCII files. It supports multiple archive groups with different frequencies and conditional archiving. Maximum and minimum values of process variables since the last disk-write are archived. A matching archive retrieval program was written and embedded into a Perl/Tk GUI with GNUplot for data display. A Web-based version of the data retriever was also developed.

For the laser control on the β-NMR experiment, LabView was used to interface to several GPIB based devices. Stabilization algorithms were developed in the hybrid EPICS/LabView system. This solution proved to be rather volatile and a major effort was launched to write EPICS device support for our Ethernet-based GPIB controllers from National Instruments.

EPICS device support for interfacing to the rf control systems was upgraded from the RFQ prototype to a more general version which adapts more easily to changes in the supervised systems.

The ISAC relational device database, which is PC based and uses Paradox, saw major enhancements during this year. Initially implemented to generate specification documents, it now stores all device parameters and hardware addresses. Reports from the database with supporting Perl scripts are now used:

- to generate system level Capfast schematics for EPICS database generation,
- to check the consistency of the interlock specifications with the software implementation in the PLC ladder logic, and
- to generate VME channel documentation on the Controls Web site.

Automatic pump-down procedures for all vacuum subsystems and improved mass-selection scripts were developed.

A hacker break-in on a SUN workstation at the ISAC ion source test stand prompted the tightening of security on all control system workstations. In addition, a Linux-based firewall was set up and tested for isolating the control system from the rest of the site. It is scheduled for final installation during the spring shutdown.

More documentation, tutorial material and troubleshooting information was added to the ISAC Controls Web site.

Commissioning and Operation

As during last year, operation consisted of a mildly chaotic mix of commissioning, upgrading, and routine running. Overall, the reliability of the control system increased dramatically. This is mainly due to resolution of PLC and IOC problems during the previous year. Another contributing factor is the increasing knowledge of the Operations group.

The CAN power supply controllers showed random, but rare, erratic behaviour, which could not be reproduced in a test set-up for a long time. After detecting higher frequency incidents at the ILE2 beam line in November, a bug-fix was applied which solved the problem. The multi-monitor console PCs running Xservers under the Windows 98 operating system proved to be barely suitable for operations and sometimes required rebooting every 8 hours. One console PC was converted to Linux on a trial basis with extremely encouraging results.

ISAC DIAGNOSTICS

Fast Faraday cups have been used to measure the longitudinal beam distribution in MEBT. One was located just before the stripping foil while the other was 3.3 m after the foil, between the charge selection slits and the drift tube linac. The narrowest FWHM measured was 0.35 ns; the rise time of the signal was 0.26 ns. At present a 2 GHz amplifier determines the bandwidth; the cups themselves are believed to be faster. The downstream cup showed clearly the increase in thickness of the stripping foil when it was bombarded by 280 nA of 0.15 MeV/u ^{20}Ne ions. The bunch centroid moved 2.5 ns after 40 minutes irradiation; this implies a reduction in energy of 24 keV, which would arise from an increase in thickness of 3 μg/cm^2. The thickening foil would increase the energy straggling and a doubling of the bunch width showed this. The transverse emittance would also increase and a reduction in beam flux on the anode was seen, consistent with beam being scattered outside the acceptance of the anode. The connector to the anode was insulated with Teflon and its low melting point limited the beam power. One needs to operate at high instantaneous currents to get reasonable signal to noise and this limitation would hinder use at the higher energies in HEBT. The design has been changed to use an SMA connector with ceramic insulation which may take between 5 and 10 W. These new cups have been installed in HEBT.

Space restrictions between tanks of the DTL meant that the ports to insert beam diagnostic instruments were only 1.25 in. longitudinally. A dc Faraday cup has been designed for this space and a slotted plate can be driven across its entrance to yield profiles of the beam in the two orthogonal directions. The EM noise is quite low, equivalent to $\sim$10 epA; however, there is also an $\sim$2 nA current of electrons from an unidentified source which may be related to the rf field and hence modulated. Capacitive pickups have been designed for this location; they have been built but not yet installed. They will be used as non-intercepting monitors of the beam phase at the commissioning currents.

Nitrogen ions were scattered from a gold foil, located at the focus of the Prague spectrometer magnet, into a silicon surface barrier detector. The detector pulses were processed to give information on beam energy and arrival time with respect to the 11.7 MHz clock referenced by the RF group. The signal processing electronics were contained in an unshielded NIM bin; the primary cables were double shielded, but the EM noise was $\pm$1.5 mV after the pre-amplifier. The ion energy was $\sim$0.23 MeV/u, i.e. 3.22 MeV, since only the first tank of the DTL was operational. The charge integrated by the pre-amplifier gave a pulse of 0.1 V with sufficient resolution for us to obtain, after correcting for kinematics, a nitrogen energy which agreed with that obtained from the known magnetic field of the spectrometer. The pre-amplifier differentiated the energy pulse to give a fast timing signal. Its amplitude was only 12 mV, and was affected by the noise. Consequently, the precision of the measurement of longitudinal distributions was only $\sim$1 ns. This was sufficient to show that the population of the weakly populated 33 MHz buckets was only 3%, and that there was no beam at this energy lying between buckets. A chopper will eventually be used to remove the sidebands. Better shielding of the electronics and a higher beam energy should improve the precision of the forthcoming measurements.

The response of most particle detectors deteriorates with prolonged exposure to beam because of changes in the surface or crystal lattice. The rate of damage caused by electrons is two or three orders of magnitude below that caused by ions. A system of tube lenses has been designed to accelerate and focus the secondary electrons produced by the passage of an ion beam through a foil onto the surface of a detector.

A ^{241}Am alpha source was used to test silicon diode detectors and a channel electron multiplier (CEM) on the bench. The CEM could be biased to repel low energy ions or electrons. It was set up first to detect alpha particles and later to detect secondary electrons created when the alpha particles hit a target. The target itself could be biased to alter the energy of the electrons accelerated into the CEM. The detection efficiency of the CEM varied across its aperture, the circumference being about half as sensitive as the centre. The response to electron energy was flatter than expected; we did not see a peak in efficiency near 1 keV as suggested by the manufacturer. The response of a microchannel plate would be more uniform over its surface, but it would share another characteristic of the CEM which is that the response is based on the secondary and tertiary electrons emitted from the surface and consequently they both respond to stray electrons and photons as well as ions. For example, the CEM counted both alpha particles and conversion electrons. Their use in beam diagnostics may therefore require electric or magnetic suppression. The response of a silicon diode detector is based on ionization throughout its bulk and the signal from a stopping ion is much greater than that from low energy electrons or photons. The background is thus much cleaner, but the signal from ions below $\sim$1 MeV is not usable.

The DRAGON team is constructing a “start” detector. This consists of a thin foil through which ions pass. A grid to accelerate secondary electrons from the back surface of the foil follows the foil. The electrons are then bent through 90° by a two grid electrostatic mirror and pass through a final grid to hit the surface of a microchannel plate (MCP). One pulse from the MCP will be used for particle identification by time of flight. Four signals from the anode behind it will provide information on the original position of the ion and these will be used to estimate its direction. A computer simulation was made of the production of the electrons and their passage was tracked through the grids to the surface of the MCP. The resolution of an image at the MCP of a point source at the foil, in space and time, was $\sigma_s \sim 2$ mm and $\sigma_t = 25$ ps. The FWHM is narrow but there are significant tails. For example, the widths at 10% of peak are 10 mm and 100 ps. This behaviour is similar to that seen at other laboratories and is caused by non-linear fields close to the grid wires.

The resolution of the MCP and anode will have to be folded with these numbers to give the resolution of the instrument, but it would appear that the timing performance should be adequate; the spatial resolution may not be. A design note has been written, DN-01-03.

A set of five independently insertable beam attenuators has been designed and drawings are being prepared for manufacture. The mechanisms insert mesh or sieve material into the beam in order to reduce the current. A sample of chemically etched sieve material with 5 μm diameter holes spaced by 50 μm has been purchased from Buckbee Mears Inc. Inspection under a microscope shows that while a few clusters of holes are occluded, the majority will transmit beam.

ISAC-II ACCELERATOR STUDIES

ISAC-II studies proceeded both on beam dynamics related issues and on hardware preparation. Beam dynamics work focused on beam simulation studies chiefly surrounding the issues of multi-charge acceleration, cavity modelling and lattice optimization. On the hardware side the prototype for the medium-β superconducting cavity was fabricated in Italy, a cryostat for cavity testing was designed locally, and efforts were made to set up a test facility at TRIUMF.

Multi-Charge Acceleration

Radioactive beam experiments in many cases are event starved. For this reason it is important that the accelerator systems are as efficient as possible. Stripping foils in accelerator systems are a necessary evil since they shorten the linac to make it economically viable, while reducing the final intensity of the beam on target by factors of 3–5. Recently the American RIA project has utilized the idea of reducing accelerator length, hence cost, by adding multiple stripping stations and maintaining beam intensity by accelerating multiple charge states. We consider here the possibility of utilizing multi-charge acceleration in the ISAC-II superconducting linac.

The linac accelerates from 0.4 MeV/u to more than 6.5 MeV/u. There will be a stripping stage at 0.4 MeV/u. It is also possible to include a second stage to (a) shorten the linac for economical reasons or (b) give flexibility to the experimenter to trade off beam energy for intensity and/or beam quality.

Figure 150 summarizes a set of possible operating modes that illustrate the benefits of multi-charge acceleration. In the model we include two stripping stages, S1 and S2, one at 0.4 MeV/u and one after the first twelve cavities or after 10 MV of effective accelerating voltage. Figure 150(a) gives the expected equilibrium charge state for stripping from each of the strippers. Stripping from S2 produces a higher charge state due to the higher incident beam velocity. Beam dynamics simulations, reported below, indicate that we can successfully accelerate particles with a relative charge difference of ∼5% in the low energy section and of ∼7% in the high energy section. These bounds give the number of possible charge states that can be simultaneously accelerated by S1 and S2. These are plotted in in Fig. 150(b). With multi-charge acceleration an experimenter could add S2 and gain a higher final energy with only minimal intensity loss. The expected final energy of the beam with two stripping foils compared to

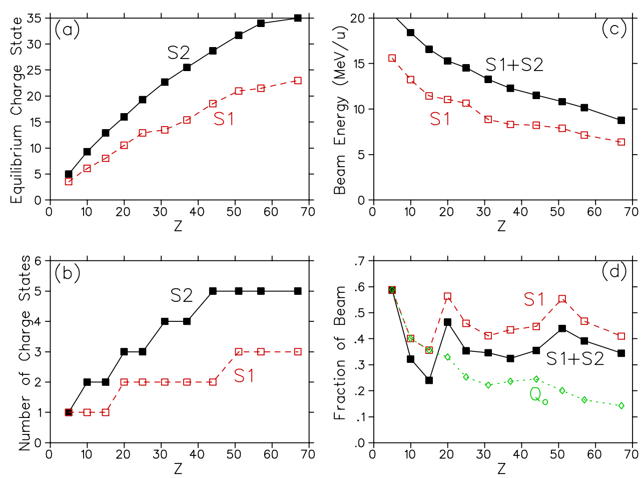

Fig. 150. Summary plots for multi-charge acceleration. Plotted in (a) are the equilibrium charge states from a carbon foil at 0.4 MeV/u and from a second foil, S2, after 10 MV of acceleration. The number of potential charge states that could be simultaneously accelerated are shown in (b). The final energies from S1 alone or S1 and S2 together are given in (c), while the acceleration efficiency for single charge acceleration (Q_o) and multi-charge acceleration with S1 and S2 are given in (d).

a single stripper, S1, is shown in Fig. 150(c). A plot of the expected acceleration efficient for the reference design case and for multi-charge acceleration with one or two stripping stages is given in Fig. 150(d). Note that even with two stripping foils the overall efficiency is improved over the single charge state case. The drawback of multi-charge acceleration is an increase in the transverse and longitudinal phase space and the increased complexity and cost of the transport and matching sections. Nevertheless, the benefits are substantial and so a beam simulation study was initiated.

Cavity modelling

Beam simulations of the superconducting linac require a definition of the field components in the cavity, so a RELAX-3D model was made of each of the three cavity types. To simplify cryostat design, all cavities have been conceptualized to have the same outer diameter. The rf frequency, beam entrance and exit tubes and inner conductor size are then selected to form a cavity geometry that will produce the design specifications. A summary of cavity specifications for the three ISAC-II superconducting cavity types are given in Table XXV.

Table XXV. Geometrical parameters of ISAC-II superconducting cavities used in the RELAX-3D modelling. Lengths in the beam direction are given for entrance and exit grounded tubes, the acceleration gaps and the inner conductor tube.

Cavity	Low	Medium	High
β (%)	4.2	7.2	10.6
f (MHz)	70.72	106.08	141.44
ID (mm)	180	180	180
Inner tube L (mm)	40	60	60
Gap L (mm)	46	40	50
Grounded tube L (mm)	24	20	10
Full bore (mm)	20	20	20

These geometric values are input into RELAX-3D to produce a static electric field distribution. The fields for all three cavity types are summarized in Fig. 151 with field values normalized to a bias of 1 V on the inner conductor. The on-axis E_z field components and the transverse field component 4 mm from the axis are given in Fig. 151(a) and (b) respectively. The asymmetry of the cavity also produces an E_y "dipole" component on-axis plotted in Fig. 151(c).

The fields are then time modulated and integrated to calculate the impact on an ion of a given velocity and phase. A summary plot of the cavity performance is shown in Fig. 152. The transit time factors for all cavities are given in Fig. 152(a). The cavities will typically be operated at a negative synchronous phase for stable longitudinal motion and this gives rise to a net transverse defocusing force and vertical steering. The

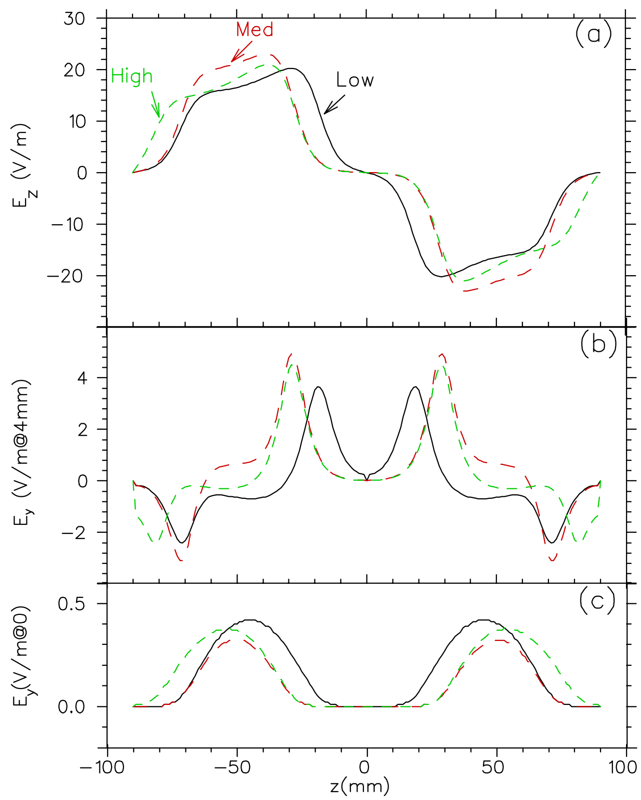

Fig. 151. The on-axis E_z field components and the transverse field component 4 mm from the axis are given in (a) and (b) respectively. The on-axis E_y component due to the cavity asymmetry is plotted in (c). All fields are normalized to a 1 V bias on the centre conductor.

defocusing focal lengths and vertical steering are plotted in Fig. 152(b) and (c) assuming a phase of $-30°$, a field gradient of 6 MV/m and an A/q of 3.

These field calculations point out the strong defocusing and steering produced in the low-β section. The latter is especially troublesome for multi-charge acceleration since the transverse phase advance per cell varies with charge so that vertical deflections on the ensemble will eventually become incoherent and lead to emittance growth. We may, as a result, alter the cavity geometry to lower the design velocity of the low-β cavity.

One-cell simulations

Initial studies of multi-charge acceleration concerned the choice of the transverse focusing lattice. The study included three kinds of transverse focusing: triplets, doublets and solenoids. The first approach was simply to consider a single non-accelerating cell made with the focusing elements separated by four accelerating cavities represented as defocusing lenses. The strength of the cavity defocusing was taken from the cavity modelling reported above. Simulations were done using the first order transport codes FLAT

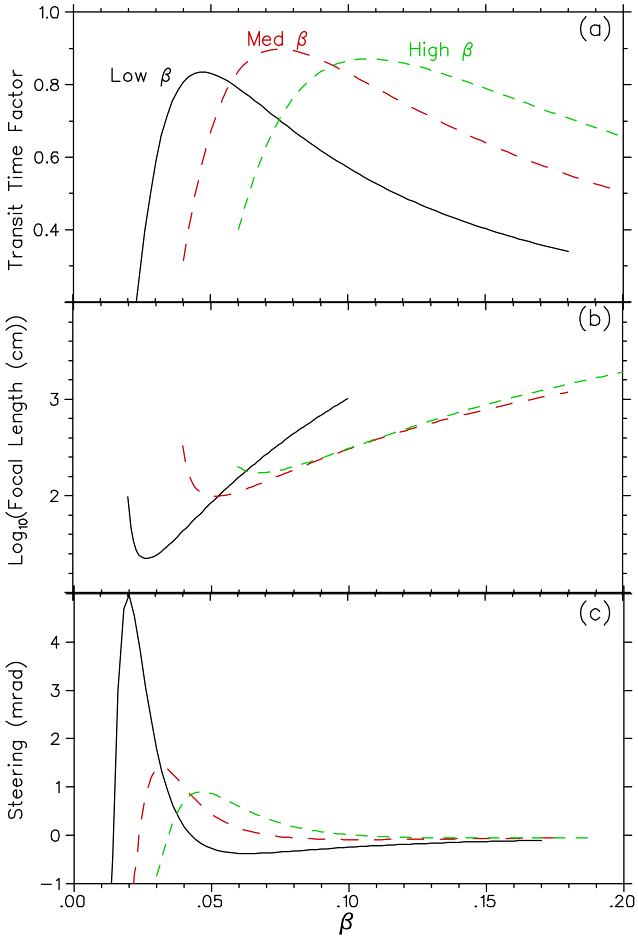

Fig. 152. (a) Gap-crossing transit time curves for the three cavities. (b) Integrated defocusing effect and (c) steering effect from a single cavity assuming 6 MV/m, $A/q = 3$, and $\phi_s = -30°$.

and TRACE3D. Lattice parameters used in the study are given in Table XXVI.

Table XXVI. Specifications for the one-cell simulations.

Parameter	Triplets	Doublets	Solenoid
A	30	30	30
q_o	5	5	5
a (cm)	1	1	1
E (MeV)	0.4/3.0/7.0	idem	idem
μ (deg)	20/40/60/80	idem	idem

Generally when two or more charges are accelerated simultaneously only one is matched to the focusing channel, the so-called *reference charge* or q_0, while all the other charges, q', will be slightly mismatched. Since the focal properties of the magnetic elements change with the charge state, each charge will undergo a different phase advance per period μ. A lattice can be characterized by envelope parameters that define the maximum beam size along the channel for a matched beam of a given emittance. For simplicity a cylindrical aperture, a, is defined and for a given emittance, ϵ, a mismatch value

$$M_{\max} = \frac{a}{\sqrt{\epsilon \beta_{\max}}}$$

can be tolerated before particles are lost, where $\beta_{\max}$ is the maximum value the β-parameter assumes along the cell. It is clear that the larger the value of $\beta_{\max}$ the lower is the mismatch factor that can be tolerated before beam loss occurs. The $\beta_{\max}$ value depends on the phase advance that is chosen for the reference charge. For each single cell calculation the phase advance for the reference particle is fixed and a matched solution for the q' charge is calculated. The two matched solutions are used to calculate a mismatch factor defined as

$$M = \sqrt{\frac{1}{2}(R + \sqrt{R^2 - 4})} - 1$$

where $R = \beta G + \gamma B - 2\alpha A$, A, B, G are the Twiss parameters for the q' ensemble and α, β, γ are the Twiss parameters for the reference particles.

Several phase advance values were studied for each lattice and for three different energy regimes corresponding to the three main sections of the linac. A phase advance near 90° was found to maximize the range of charge that can be transported within the lattice bore. Figure 153 gives the range of charge states that can be successfully transported for each lattice type as a function of energy. The range of transported charge is very narrow in the low energy section where the high cavity defocusing results in large values of $\beta_{\max}$. It should be noted that the simpified study does not differentiate between magnet bore and linac bore sizes, as would occur in a typical linac.

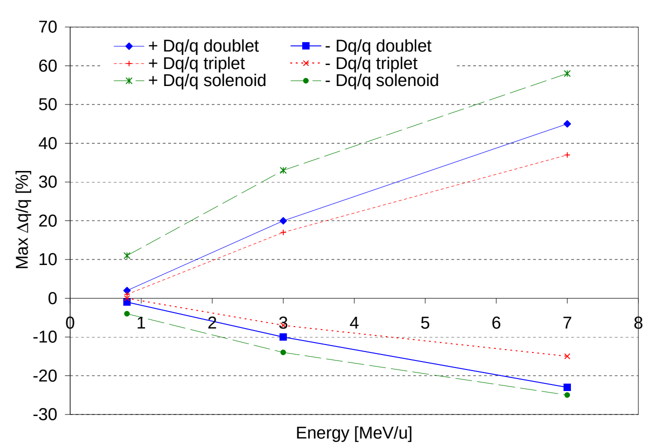

Fig. 153. Different charge transported for the three lattices and at different energies.

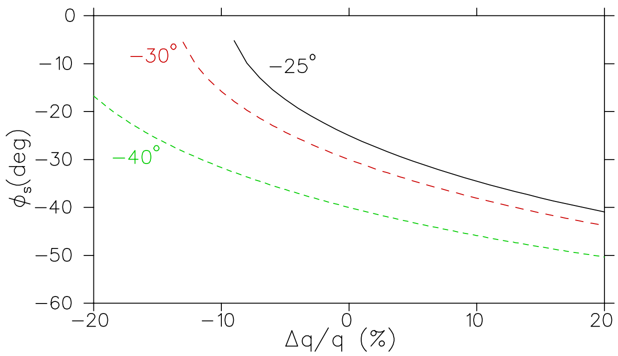

Fig. 154. The synchronous phase associated with various $\Delta Q/Q$ values for three different q_0 synchronous phases.

Longitudinal motion

In longitudinal phase space the reference particles are accelerated with a constant negative synchronous phase, ϕ_{so}, while other charges, q', oscillate around a different synchronous phase, $\phi_{s'}$. A plot of $\phi_{s'}$ values as a function of $\Delta Q/Q$ assuming ϕ_{so} values of $-25°$, $-30°$, and $-40°$ is given in Fig. 154. Longitudinal motion will be stable within a certain band of q' values, though emittance growth of the particle ensemble will result due to the different oscillation amplitudes and phase advance of the constituent charges.

Beam simulations

Each of the three lattices was studied with the multi-particle code LANA. Beams of initial emittance $\epsilon_{x,y} = 0.15$ π mm-mrad normalized and $\epsilon_z = 3$ π keV/u-ns for $A/q = 7$ were simulated using triplets, doublets or solenoids between cryostats. The longitudinal emittance is chosen to be a factor of three larger than the expected emittance to test the lattice acceptance. Each simulation was performed with 5000 particles. The linac specifications for this study are given in Table XXVII.

Table XXVII. Specifications for the linac structure.

Parameter	Low-β	Mid-β	High-β
A/q	7	7	7
β_0	4.2	7.2	10.5
E (MeV/u)	0.4 – 1.3	1.3 – 4.0	4.0 – 6.5
freq. (MHz)	70	105	140
$N_{\rm cav}$	8	20	20
$N_{\rm cryo}$	2,4[1]	5	5
E_g (MV/m)	5	6	6

Satisfactory solutions were found for each of the three cases. It is found that minimizing the intertank length is crucial for improving longitudinal acceptance and reducing the emittance growth in multi-charge mode. In the doublet case it is necessary to increase the focusing for the first eight cavities to a doublet between every two cavities. The transverse envelopes for the single charge state mode for the triplet, doublet and solenoid cases are given in Figs. 155, 156 and 157 respectively. Transverse and longitudinal emittance growth are less than 20% in all cases, with the solenoid case the superior of the three.

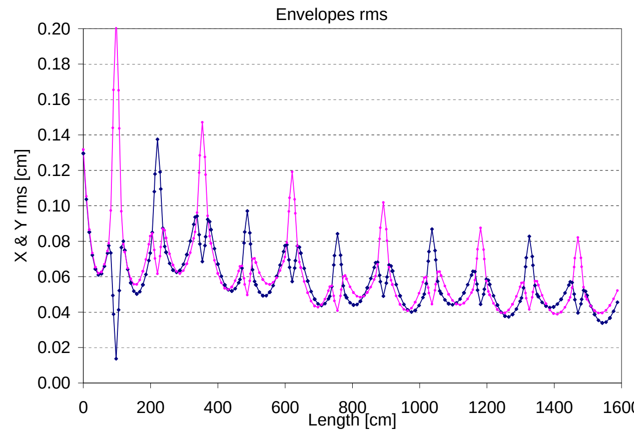

Fig. 155. Transverse envelopes for a single charge state in the linac with triplet focusing.

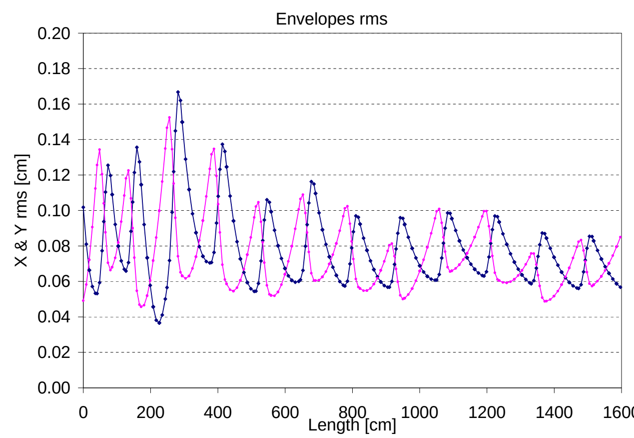

Fig. 156. Transverse envelopes for a single charge state in the linac with doublet focusing.

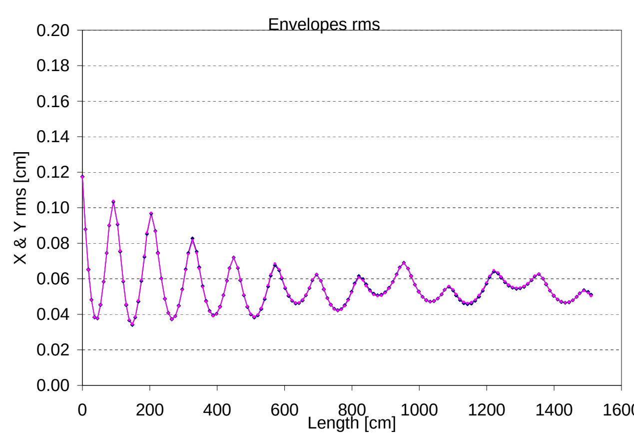

Fig. 157. Transverse envelopes for a single charge state in the linac with solenoid focusing.

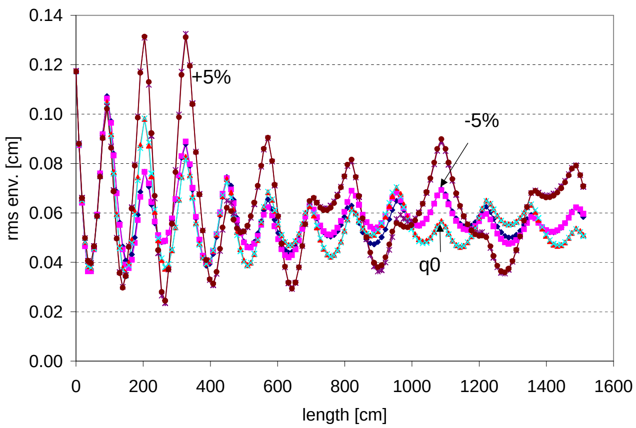

Fig. 158. Transverse envelopes for each of $\Delta q/q = -5, 0, 5\%$ and initial displacement of 500 μm in the linac with solenoid focusing.

Multi-charge simulations were done by fixing the linac parameters for the q_o case and altering the charge of the initial beam. Mis-alignment sensitivity was simulated by shifting the initial beam position by 0.5 mm in both x and y. Beam envelopes for a multi-charge run through the solenoid focused linac are given in Fig. 158. The six curves correspond to x and y envelopes for each of $\Delta q/q = -5, 0, 5\%$. In general the longitudinal dynamics proves to be more restrictive than the transverse dynamics for all cases. Figure 159(top) shows the final position in longitudinal phase space of seven charges accelerated through the solenoid case.

Ensembles of individual charge states experience relatively little growth except near the extremes of $\Delta Q/Q$ but the enfolding ellipse is 7 times larger; 20 π keV/u-ns over the single charge state value of 3 π keV/u-ns. The emittance of the transverse ensemble in the solenoid case for $\pm5\%$ charge difference and 500 μm centroid shift is shown in Fig. 159(bottom). The enfolding ellipse increases from 0.15 π mm-mrad to 0.4 π mm-mrad over the single charge state performance. The transverse acceptance of the triplet and doublet case is less than in the solenoid case for displaced beams.

Future work will involve installing the realistic fields inside LANA to better simulate the transverse motion and to design matching and transport beam lines compatible with multi-charge acceleration.

Hardware Studies

The specification of the superconducting linac calls for three cavity types of frequency (β_o) 70.7 MHz (4.2%), 106.1 MHz (7.2%) and 141.4 MHz (10.5%) respectively. A medium-β quarter wave bulk niobium cavity has been designed and fabricated in collaboration with INFN-Legnaro. The cavity is shown in Fig. 160 along with some design parameters. Signal

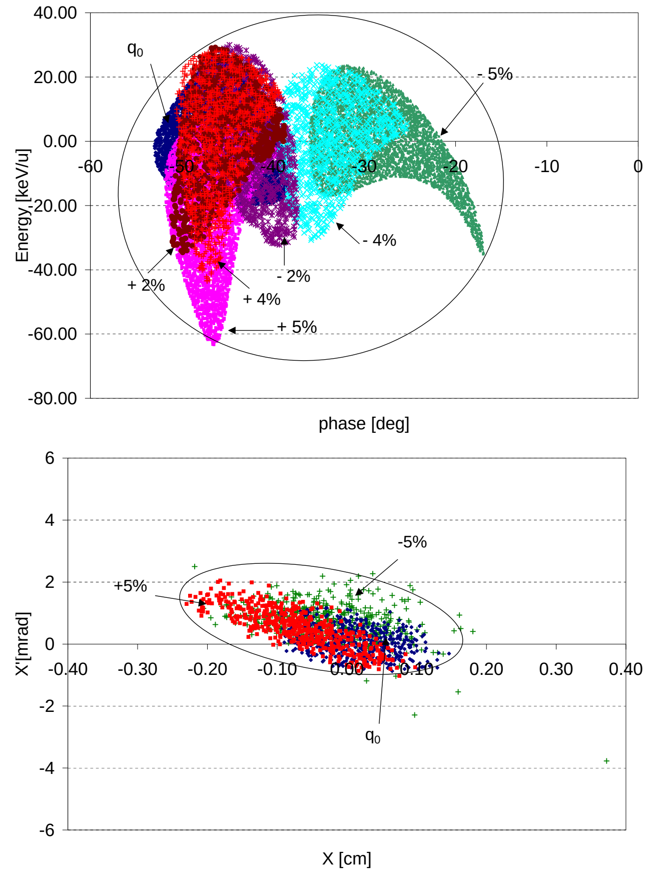

Fig. 159. Top) Final longitudinal position of seven different charge states after acceleration through the linac with solenoid focusing. The enfolding ellipse for the whole ensemble is highlighted. Bottom) Final transverse position of three different charge states with initial displacement of 500 μm after acceleration through the linac with solenoid focusing. The enfolding ellipse for the whole ensemble is highlighted.

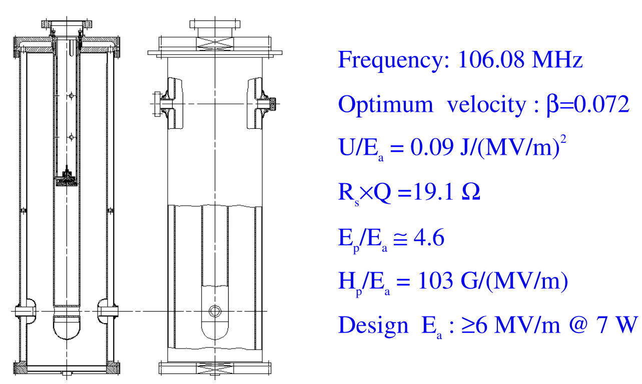

Fig. 160. The prototype 106.1 MHz medium-β cavity for the ISAC-II project at TRIUMF.

level tests were completed at Legnaro to confirm the frequency. The cavity will receive chemical polishing at CERN followed by rf tests in Legnaro with delivery to TRIUMF expected in late spring, 2001.

A superconducting rf test lab is now being planned at TRIUMF. RF testing equipment has been itemized and ordered. A single cavity test cryostat has been designed in a collaboration between TRIUMF and Quantum Technology of Whistler. The cryostat includes a large cylindrical vacuum vessel with top flange, a removable liquid nitrogen shield vessel, a top cold shield, a lower radiation baffle, a liquid helium reservoir, and a μ-metal shield. Several new ancillary devices are in the process of being prototyped for the superconducting rf development program. They include a combined coarse and fine tuner composed of a mechanical lever and a Piezo crystal and an rf coupler. A "dummy" copper model of the medium-β prototype is being manufactured at TRIUMF to aid in the development of the rf controls and ancillary equipment.

ISAC PLANNING

This year the Planning group was involved in planning, scheduling, coordinating and expediting several sub-projects for ISAC.

Various plans and PERTs were prepared and updated regularly with manpower estimates and analysis to identify critical areas and resolve any problems. ISAC priorities were evaluated and higher priority was assigned to: the consolidation of MRO and essential projects in the target area to increase beam reliability; completion of a hot cell; completion of β-NMR for the first experiment in May, and for the soft landing experiment with the high voltage cage in July.

On the accelerator side, the major milestones included: Test #2 (commission MEBT) by February; Test #3 (commission beam from DTL tank 1 including triplet and buncher) by July; and install all DTL systems and accelerate beam to 1.5 MeV/u by December. Manpower planning was done, activities were coordinated and expedited through the Design Office and Machine Shop, and the above goals were achieved on schedule.

Technical details and progress on PERTed activities are described elsewhere in this report under the respective principal group. However, following is a summary of the main projects along with the major milestones achieved.

Target Areas and Hot Cells

Extensive work was done to upgrade target areas, target hall crane interlocks and controls, hot cell (improved system for lead glass shielding windows, portable shielding plug, and access doors). Other work included: ITW5B and associated new iron and concrete shielding; DB0 redesign; ECR source; target module updates. Some contamination was experienced while changing a target, which increased the priority of designing a decontamination facility. An alternative conditioning system to expedite the process of changing ISAC targets was designed and fabrication is in progress.

MEBT

After completing Test #1 of MEBT up to DB5, installation of the MEBT was finished and Test #2 was completed on schedule in February. This test included both benders, diagnostics systems, slits, collimators, controls, the charge selection slit system (DB7), stripper foil in MEBT, and installation of a diagnostic station and emittance rig with necessary diagnostics system. The 35 MHz rebuncher was not installed for Test #2 and the MEBT chopper had to be deferred until March, 2001 due to higher priority on DTL systems.

DTL Systems

After evaluating the priorities and workload, it was decided to do Test #3 with DTL tank 1, triplet and buncher in June to gain experience and then install and test all DTL systems to accelerate the beam to 1.5 MeV/u in December. One large stand was designed, fabricated and installed in March to support all 5 DTL tanks.

Fabrication of DTL tanks 2 to 5 with stems and ridges was done in July, followed by assembly, rf tests and preparations for installation in the ISAC hall. Additional time had to be spent on installing extra cooling for tanks 2–5 after encountering problems during power tests of tank 2. Consequently only tanks 2, 3 and 4 were tested to full power in the bunker in the proton hall extension before moving to the ISAC hall with a plan to do power tests for tank 5 *in situ*. Vacuum through all DTL systems was achieved by December 15, and a helium beam from the off-line source was accelerated to 1.5 MeV/u on December 21.

HEBT

Due to increased workload, the HEBT project was divided into two parts: HEBT1 (up to upstream of benders to DRAGON and TUDA beam lines) and HEBT2 (all remaining HEBT components). Major jobs included: design, fabrication and installation of vacuum system, beam line hardware, diagnostics, and controls components for HEBT1 to commission beam through all DTL systems. HEBT1 commissioning required installation of the Prague magnet and diagnostic station with all commissioning diagnostics. Due to the heavy workload in the ISAC RF group, all rf activities had to be carefully planned, coordinated and expedited. The 11 MHz buncher, chopper and bunch rotator had to be deferred until spring, 2001 due to the higher priority on accelerating beam through DTL tank 5 to 1.5 MeV/u in December. Chalk River quads were mapped and installed and all four benders were also installed and aligned by early December.

Low Energy Experiments

These included essential modifications to GPS (lifetime), LTNO, yield station, and β-NMR. Extensive work was done on planning, coordinating and expediting activities and critical components from the Machine Shop and outside suppliers for β-NMR, laser polarization systems, spectrometer, and associated LEBT components. The first β-NMR experiment in 2000 was done in May, followed by installation of the HV cage with associated safety control systems to do a soft landing experiment in July, and then another in November with an aim to increase polarization.

High Energy Experiments

These involved DRAGON and TUDA. Installation of HEBT components up to the TUDA experimental station, with associated services, started with an aim to finish before March, 2001. A special room was designed and constructed for the TUDA detector system electronics, with all services and a special grounding system. The plan was to be ready for stable beam tests by the end of March, 2001.

DRAGON

In spite of significant efforts in the Design Office, overall progress on DRAGON was relatively slow due to a lack of resources and a higher priority on DTL and HEBT tests. All major components for legs 1–5 were installed by the end of September, and services were connected by December. ED1 and ED2 tanks were installed and electrodes assembled in September, and the tank vacuum tested in October/November. Magnetic dipoles (MD1 and MD2) were installed and the MD1 vacuum chamber was fabricated and made ready for installation. Several initial tests were done to commission the gas target with the control system. The plan is to be able to start α particle tests up to the charge slits by January, and continue these tests down the line as services are completed, with a goal of being ready for stable beam by April, 2001.

ISAC-II

PERTs were prepared that included work on specifications and design of a superconducting rf test facility and dummy cavity with an aim to install and test a Nb cavity in summer, 2001 after receiving it from Legnaro.

CONTRACT ADMINISTRATION

In the past year eight major contracts were awarded:

- Sunrise Engineering Ltd. of B.C. manufactured the DRAGON electrostatic dipole tanks, and Swiss Wire (EDM) of California manufactured the DRAGON electrostatic dipole electrodes.
- Sunrise Engineering Ltd. of B.C. manufactured DTL tanks 2, 3, 4 and 5.
- Sunrise Engineering Ltd. also made the HEBT 22.5° dipole magnet poles and assembled the magnets, with Danfysik A/S of Denmark supplying the magnet coils.
- Performance Development Ltd. of B.C. manufactured the 51 stems for DTL tanks 2, 3, 4 and 5.
- Sunrise Engineering Ltd. of B.C. manufactured the HEBT 35 MHz buncher tank.
- Sunrise Engineering Ltd. also fabricated the spent target storage tank for the ISAC target hall.

Personnel Resources

In 2000 the average monthly personnel effort for ISAC increased by approximately 4.5 people to an average of 83.75 FTE people per month (see Fig. 161). In 1999 the FTE effort per month was 79.25 people.

In 2000 the average monthly personnel effort per system was as given in Table XXVIII and shown in Fig. 162.

Table XXVIII. Personnel effort per system.

System	Monthly FTE
Project management & administration	3.44
Beam line 2A	0.75
Target station	5.43
LEBT	7.00
Accelerator	17.12
Science facilities (TRIUMF personnel)	21.02
Science facilities (non-TRIUMF personnel)	2.10
Infrastructure	9.43
Integration	16.89
ISAC-II	0.57
Total average FTE monthly personnel	83.75

Figure 163 shows the average monthly FTE personnel working on ISAC for the year 2000 based on the type of personnel. The average monthly FTE personnel effort spent on ISAC science for the year 2000 is shown in Figure 164.

The total personnel effort for ISAC since the start of the project January 1, 1996 to December 31, 2000 has been 346.62 years of work, based on a FTE work-month of 150 hours per person.

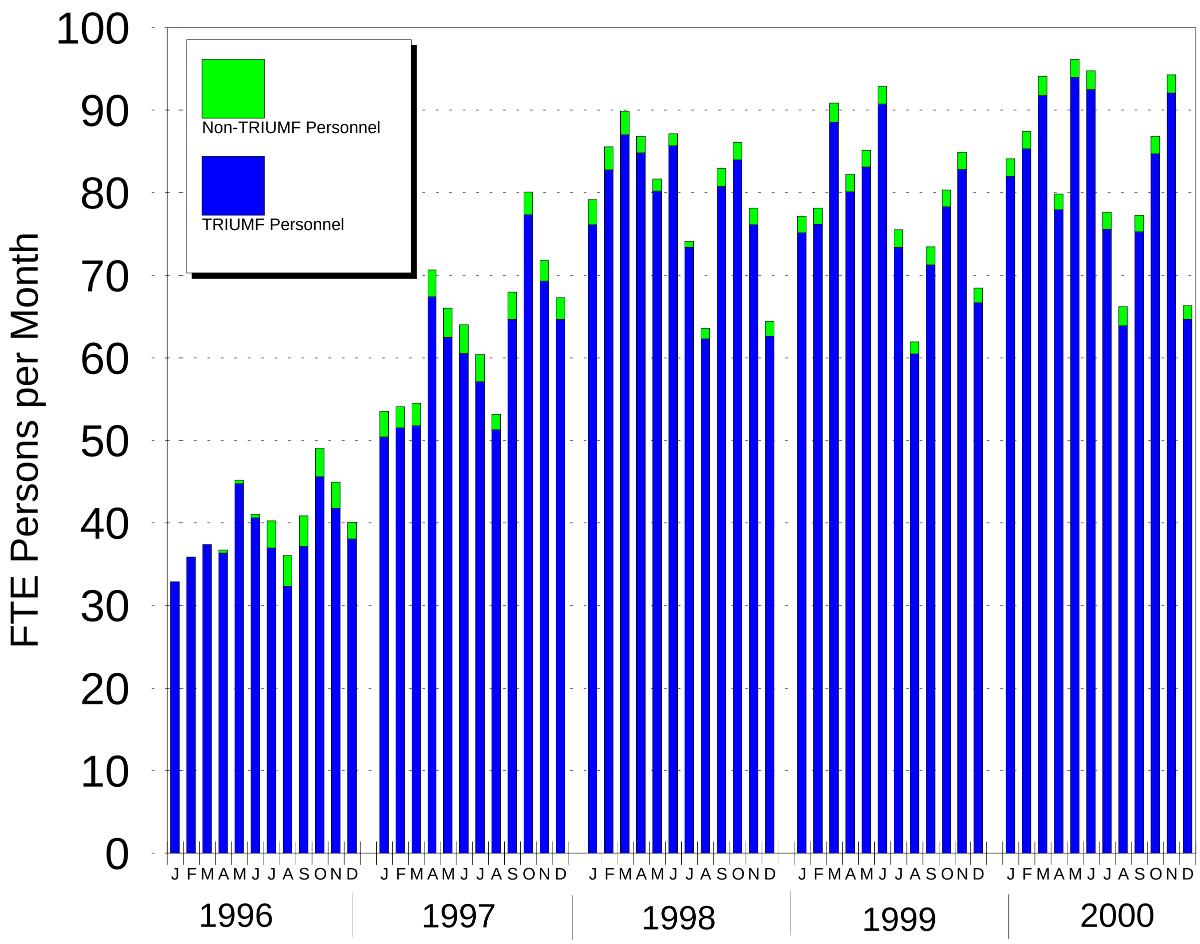

Fig. 161. ISAC monthly personnel effort, January 1, 1996 to December 31, 2000.

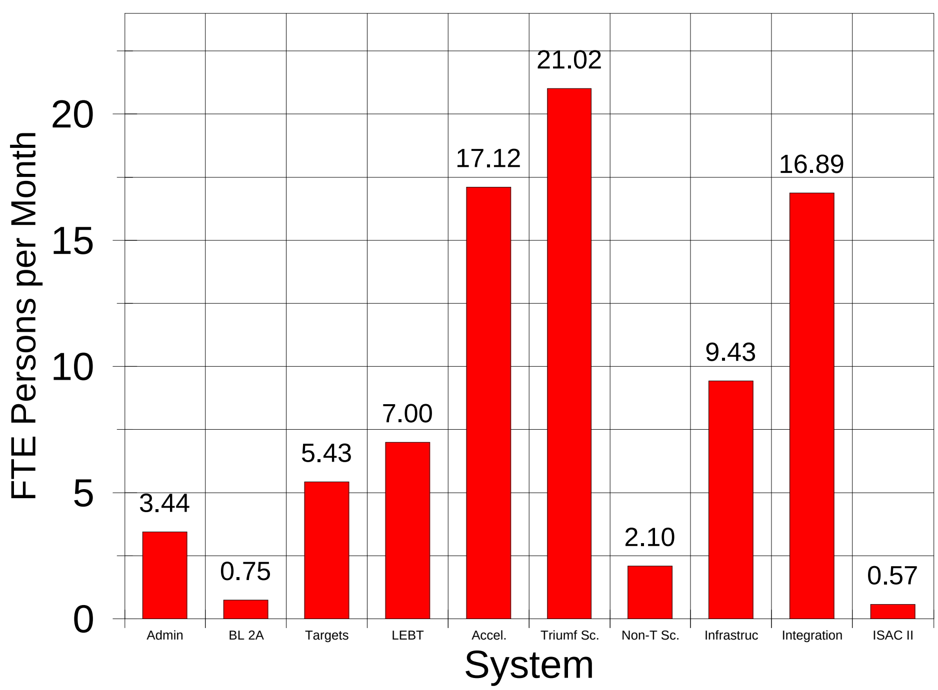

Fig. 162. ISAC average monthly personnel effort, shown by system for 2000.

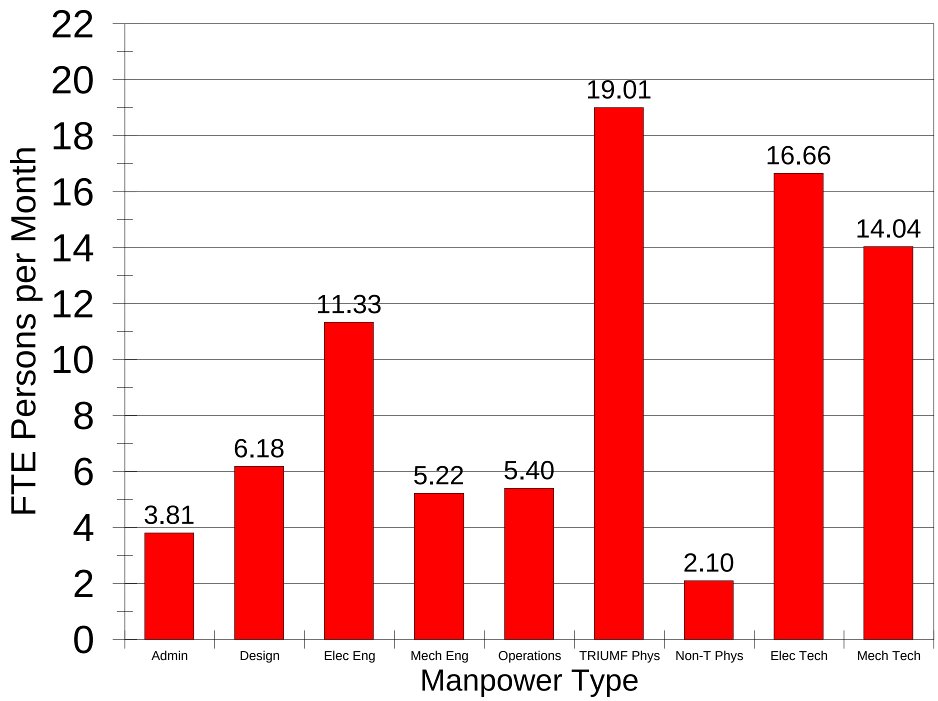

Fig. 163. ISAC average monthly personnel effort, shown by personnel type for 2000.

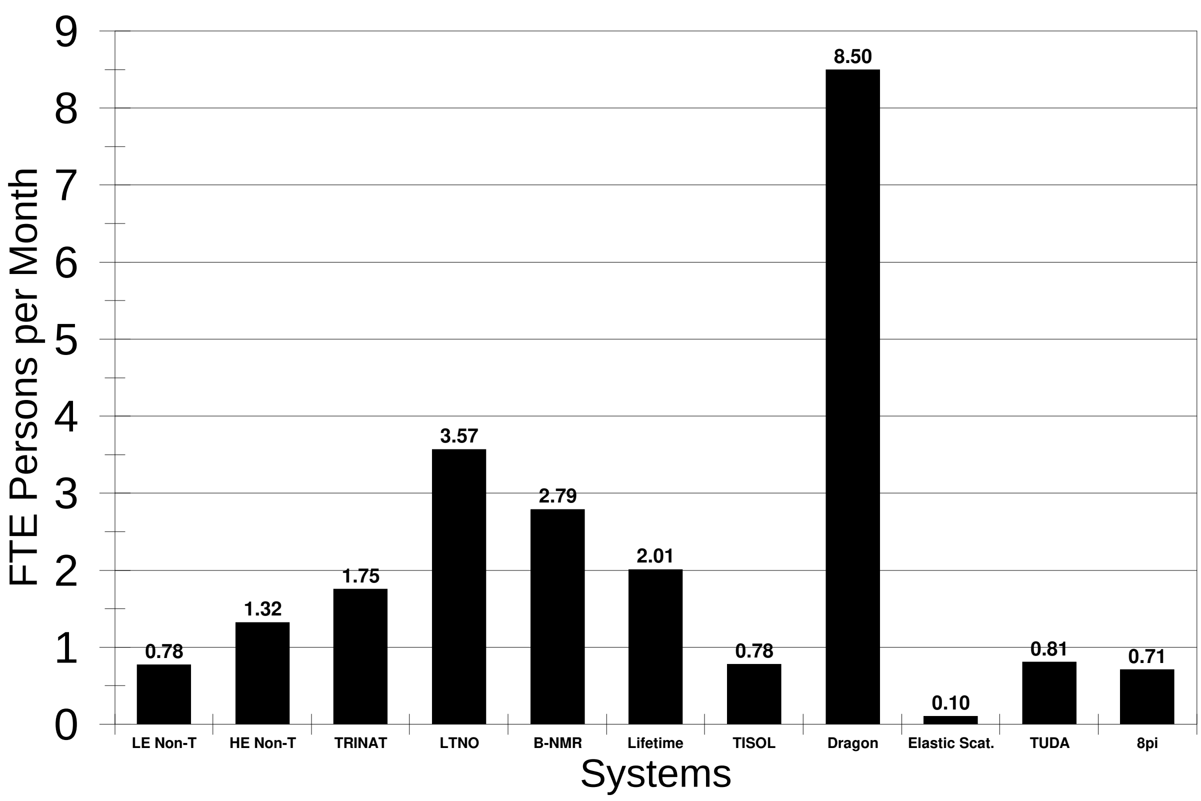

Fig. 164. ISAC average monthly personnel effort, science facilities for 2000.